Exploring Listeria monocytogenes transcriptomes in correlation with divergence of lineages and virulence as measured in Galleria mellonella

Bo-Hyung Lee, Dominique Garmyn, Laurent Gal, Cyprien Guerin Guérin, Laurent Guillier, Alain Rico, Björn Rotter, Pierre Nicolas, Pascal Piveteau

AMERICAN SOCIETY FOR MICROBIOLOGY | Applied and Environmental Microbiology®

FOOD MICROBIOLOGY

Exploring *Listeria monocytogenes* Transcriptomes in Correlation with Divergence of Lineages and Virulence as Measured in *Galleria mellonella*

Bo-Hyung Lee,[a,f]* Dominique Garmyn,[b] Laurent Gal,[b] Cyprien Guérin,[c] Laurent Guillier,[d] Alain Rico,[e] Björn Rotter,[f] Pierre Nicolas,[c] Pascal Piveteau[b]

[a]École Doctorale des Sciences de la Vie, Université Clermont Auvergne, Santé, Agronomie, Environnement, Clermont-Ferrand, France
[b]Agroécologie, AgroSup Dijon, Institut National de la Recherche Agronomique (INRA), Université Bourgogne Franche-Comté, Dijon, France
[c]Mathématiques et Informatique Appliquées du Génome à l'Environnement, INRA, Université Paris-Saclay, Jouy-en-Josas, France
[d]French Agency for Food, Environmental and Occupational Health & Safety (Anses), Laboratory for Food Safety, Maisons-Alfort, France
[e]Thermo Fisher Scientific, Villebon-sur-Yvette, France
[f]GenXPro GmbH, Frankfurt am Main, Germany

ABSTRACT As for many opportunistic pathogens, the virulence potential of *Listeria monocytogenes* is highly heterogeneous between isolates and correlated, to some extent, with phylogeny and gene repertoires. In sharp contrast with copious data on intraspecies genome diversity, little is known about transcriptome diversity despite the role of complex genetic regulation in pathogenicity. The current study implemented RNA sequencing to characterize the transcriptome profiles of 33 isolates under optimal *in vitro* growth conditions. Transcript levels of conserved single-copy genes were comprehensively explored from several perspectives, including phylogeny, *in silico*-predicted virulence category based on epidemiological multilocus sequence typing (MLST) data, and *in vivo* virulence phenotype assessed in *Galleria mellonella*. Comparing baseline transcriptomes between isolates was intrinsically more complex than standard genome comparison because of the inherent plasticity of gene expression in response to environmental conditions. We show that the relevance of correlation analyses and their statistical power can be enhanced by using principal-component analysis to remove the first level of irrelevant, highly coordinated changes linked to growth phase. Our results highlight the major contribution of transcription factors with key roles in virulence to the diversity of transcriptomes. Divergence in the basal transcript levels of a substantial fraction of the transcriptome was observed between lineages I and II, echoing previously reported epidemiological differences. Correlation analysis with *in vivo* virulence identified numerous sugar metabolism-related genes, suggesting that specific pathways might play roles in the onset of infection in *G. mellonella*.

IMPORTANCE *Listeria monocytogenes* is a multifaceted bacterium able to proliferate in a wide range of environments from soil to mammalian host cells. The accumulated genomic data underscore the contribution of intraspecies variations in gene repertoire to differential adaptation strategies between strains, including infection and stress resistance. It seems very likely that the fine-tuning of the transcriptional regulatory network is also a key component of the phenotypic diversity, albeit more difficult to investigate than genome content. Some studies reported incongruity in the basal transcriptome between isolates, suggesting a putative relationship with phenotypes, but small isolate numbers hampered proper correlation analyses with respect to their characteristics. The present study is the embodiment of the promising approach that consists of analyzing correlations between transcriptomes and various isolate characteristics. Statistically significant correlations were found with

Citation Lee B-H, Garmyn D, Gal L, Guérin C, Guillier L, Rico A, Rotter B, Nicolas P, Piveteau P. 2019. Exploring *Listeria monocytogenes* transcriptomes in correlation with divergence of lineages and virulence as measured in *Galleria mellonella*. Appl Environ Microbiol 85:e01370-19. https://doi.org/10.1128/AEM.01370-19.

Editor Edward G. Dudley, The Pennsylvania State University

Address correspondence to Pierre Nicolas, pierre.nicolas@inra.fr, or Pascal Piveteau, piveteau@u-bourgogne.fr.

* Present address: Bo-Hyung Lee, Virologie et Immunologie Moléculaires, INRA, Jouy-en-Josas, France.

P.N. and P.P. contributed equally to this work.

Received 20 June 2019
Accepted 25 August 2019
Accepted manuscript posted online 30 August 2019
Published 16 October 2019

phylogenetic groups, epidemiological evidence of virulence potential, and virulence in *Galleria mellonella* larvae used as an *in vivo* model.

KEYWORDS *Galleria mellonella*, *Listeria monocytogenes*, lineage, transcriptomics, virulence

The genus *Listeria* currently groups 20 species among which *Listeria monocytogenes* and *Listeria ivanovii* are considered pathogenic (1, 2). *L. monocytogenes* is found in a wide range of habitats, including soil, vegetation, water, and food processing environments, and as a facultative intracellular pathogen in mammal and nonmammal hosts (3, 4). This bacterium also stands as an important model to study host-pathogen interactions (5). In humans, *L. monocytogenes* is the causative agent of listeriosis, a foodborne disease resulting from ingestion of contaminated food products, especially ready-to-eat foods (6). Symptoms of listeriosis range from none to febrile gastroenteritis in healthy people to meningitis, meningoencephalitis, and septicemia with a high fatality rate in immunocompromised individuals. In pregnant women, perinatal infections can lead to miscarriage, stillbirth, or premature birth (7).

Isolates of *L. monocytogenes* are classified into four phylogenetic lineages. Most isolates belong to lineage I (serotypes 4b, 1/2b, 3b, 4d, 4e, and 7) and lineage II (serotypes 1/2a, 1/2c, 3a, and 3c), while lineages III and IV (serotypes 4a, 4c, and 4b) appear to be smaller groups. Overrepresentation of serotypes 1/2a, 1/2b, 1/2c, and 4b is observed in food and clinical isolates, and serotype 4b accounts for the majority of cases of listeriosis in humans (8, 9). Additionally, multilocus sequence typing (MLST) unravelled clonal structure (10) as well as the uneven distribution of clonal complexes (CCs) in clinical and food isolates in which hyper- and hypovirulent clones were further identified (11, 12).

To date, all *L. monocytogenes* isolates are considered to be equally virulent by governmental and international food safety authorities such as the European Food Safety Authority in the European Union and the Food and Drug Administration in the United States. However, it is contradicted by accumulating evidence (11, 13). The virulence of *L. monocytogenes* is determined by its capacity to circumvent innate host barriers such as microbiota (14, 15) and its ability to hijack host cell functions during its intracellular life cycle (5, 16). The onset of infection relies on expression of virulence factors (17), many of which are clustered in the *Listeria* pathogenicity islands (LIPIs), whose distribution is phylogenetically distinctive (11, 18, 19). The 9-kb chromosomal LIPI1 contains *prfA*, *plcA*, *hly*, *mpl*, *actA*, and *plcB* encoding the key virulence factors required for intracellular lifestyle (19). Additional pathogenicity islands (11, 20), antibiotic resistance plasmids (21, 22), and a plasmid carrying an internalin gene (23) were reported as additional virulence determinants. Moreover, reports on the direct and indirect involvement of several small noncoding RNAs in pathogenesis have increased over the last decade (24–27).

A range of molecular markers were proposed to approximate the virulence potential of *L. monocytogenes* isolates (28–30) on the basis of genomic analysis. As an example, detection of point mutations in *inlA* was tested to predict noninvasive isolates (31). Similarly, multiplex PCR detecting *inlA*, *inlC*, and *inlJ* as biomarkers was proposed to assess virulence potential (32). However, because of the high degree of intraspecific genetic diversity and the complex mechanisms leading to infection in the host, estimating virulence by analyzing a discrete number of genes may yield unsatisfactory results (33, 34). Moreover, a recent study showing epistatic control of fosfomycin resistance by *prfA* and *hpt* during infection supports complex genotype-phenotype associations (35).

In parallel to genome diversity studies, transcriptome profiling evidenced global transcriptional reshaping during infection, and a large set of virulence-associated genes were identified (24, 36). A complex network of transcription factors tightly coordinates virulence-related gene expression. PrfA, the master activator of virulence factors, the alternative sigma factor B (σ^B), the major regulator of stress responses, AgrA, the

response regulator of the Agr system, and several noncoding RNAs are part of this regulatory network (25, 37–39).

Importantly, several studies reported differential expression of conserved genes between pathogenic versus nonpathogenic isolates (40–43) which could reflect the contribution of the regulatory network to fine-tuning gene expression of virulent isolates immediately after ingestion and in the gastrointestinal tract, therefore maximizing their fitness in the host system (44). However, as most studies were restricted to a limited number of strains, the weight of intraspecific diversity tended to be overlooked. To overcome this limitation, a collection of 91 phylogenetically divergent isolates from diverse origins were processed in the *Galleria mellonella* virulence assay in order to compare their virulence potential. A subset of 33 isolates was then analyzed by high-throughput RNA sequencing (RNA-seq) to explore transcriptome heterogeneity according to phylogenetic distance and virulence potential.

RESULTS

Intraspecific virulence phenotype monitored in the *G. mellonella* virulence assay. The virulence of a collection of 91 isolates was assessed using the *G. mellonella* virulence assay. Inoculums were prepared from early stationary-phase cultures in order to limit variability in cell numbers and overall growth stage between experiments, considering the large number of isolates under study. To verify the relevance of the protocol, the bacterial loads used for assays of the first 63 isolates were compared (see Table S1 in the supplemental material). CFU ranged from a minimum of 0.70×10^6 to a maximum of 2.37×10^6 with a mean value of 1.53×10^6 and standard deviation of 0.35×10^6. Grubb's test identified no outliers, and D'Agostino-Pearson omnibus normality test did not reject normality ($k2 = 0.711$, $P = 0.701$) suggesting that the numbers of injected bacteria were comparable between isolates. Survival of larvae postinfection was monitored daily, and the time (in days) needed to kill more than 50% of the insects (LT50) was calculated. All isolates were capable of killing larvae, but their observed LT50s varied greatly (Fig. 1). While one isolate killed more than 50% of larvae within the first 24 h postinfection (LT50 of 1), eight isolates did not reach 50% death by 5 days postinfection (LT50 of >5, encoded as 6). A majority of isolates (72.4%) showed LT50s of 2 to 3 days (37 and 28 isolates, respectively). The rest showed LT50s of 4 and 5 days (8 and 9 isolates, respectively).

The 89 isolates with known lineage were grouped according to their LT50s (Table 1). No significance (Fisher's exact test, $P = 0.93$) was observed, implying no association between lineage and LT50 measured in *G. mellonella*. Similarly, no relation was found ($P = 0.83$) between LT50 values and epidemiological backgrounds (i.e., epidemic, fecal, or food-related samples).

On the basis of LT50 grouping, a subcollection of 33 isolates was selected to explore the diversity of transcriptomes of *L. monocytogenes*. Three criteria were taken into consideration in selecting these isolates: even coverage of LT50 groups measured in *G. mellonella*, representation of lineage II versus lineage I, and CC-based virulence level. The latter, hereafter referred to as Maury's classification, establishes three CC-based virulence groups (hypovirulent, intermediate or unknown, and hypervirulent) based on a comprehensive analysis of population clonal structure in relation to isolates' origin and further *in vivo* assay confirmation (11). Figure 2 shows the three classifications superimposed onto a phylogenetic tree reconstructed after complete genome comparison of the 33 isolates. This representation highlights the tight connection between Maury's classification and lineage, since all genotypes of hypervirulence (CC1, CC2, CC4, and CC6) were closely distributed in lineage I, while those of hypovirulence (CC9 and CC121) were grouped in lineage II.

Exploratory analysis of transcriptomes. (i) Global variations in transcript expression and PCA analysis. A total of 66 transcriptome profiles were obtained from duplicated exponential cultures of 33 isolates grown in brain heart infusion (BHI) broth at 37°C, as previously proposed to best mimic intracellular growth (36). Transcript levels of 2,456 conserved single-copy genes demonstrated large variations across samples

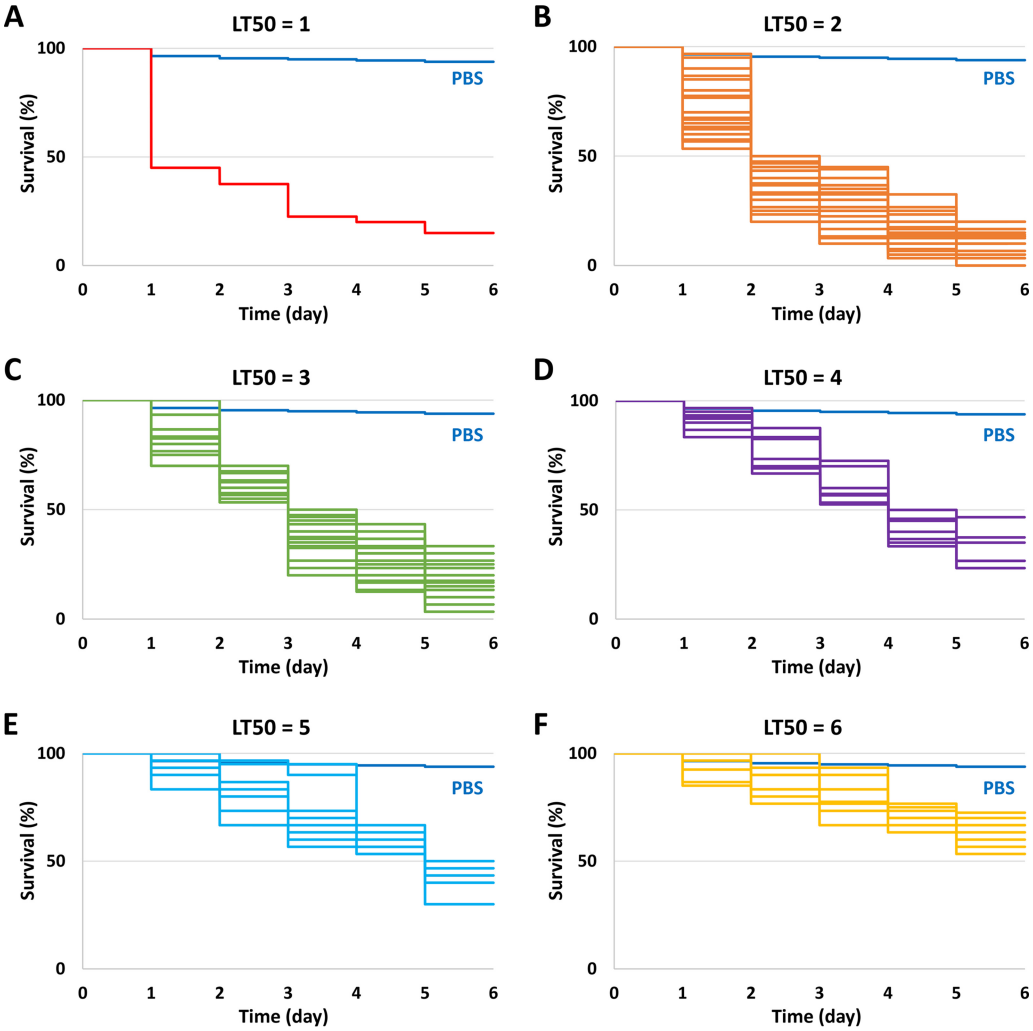

FIG 1 Virulence levels of 91 *L. monocytogenes* isolates in *G. mellonella*. Isolates are grouped by postinfection incubation time (in days) required to observe 50% or more death of larvae (LT50). Larvae injected with PBS served as negative controls. Panels A to E show isolates with LT50 of 1 to 5 days, respectively, and panel F shows isolates that did not reach 50% death by day 5 postinfection (LT50 of >5, encoded as 6).

which delineated groups of genes with highly correlated expression profiles (left dendrogram in Fig. 3A). Intriguingly, transcriptome profiles were not always consistent between duplicates, suggesting sources of variability that may complicate comparisons between isolates. To further investigate the patterns of variations, principal-component analysis (PCA) was applied to project the 66 transcriptomes, each characterized by the levels of 2,456 transcripts, onto spaces of smaller dimensions. It revealed that coordinates of the samples on a single axis (the first of the PCA, hereafter referred to as principal-component axis 1 [PC1]) was able to explain 48.4% of the total variance. Figure 3B shows that PC1 identified the existence of a continuum of transcriptome profiles that was not directly connected to the isolates' characteristics.

To understand the source of this heterogeneity, the genes that contributed the most to PC1 were checked for their functional category. Loading values for PC1 were calculated for each gene, and 100 genes positioned at both extreme positive and negative ends of PC1 were examined for the distribution of functional categories (Fig. 4). Functions involved in exponential growth (e.g., "Cell division," "RNA synthesis," and "Protein synthesis") were negatively linked with position on PC1. On the other hand, functions related to the transition to stationary phase were positively linked with position on PC1 (e.g., "Intermediary metabolism," "Adaptation to atypical conditions,"

TABLE 1 Characteristics of *L. monocytogenes* strains used in this study

Lineage[a] and MLST	Maury's classification[b]	LT50 (days)	RNA-seq[c]	Origin[d]	Isolate (reference)
Lineage I					
CC1	+	3		Sporadic	H14 (29)
CC1	+	2		Sporadic	H21 (29)
CC1	+	2		Sporadic	H22 (29)
CC1	+	2		Epidemic	H36 (29)
CC1	+	3	Yes	Food	2-11 (75)
CC1	+	2		Food	2-12 (75)
CC2	+	3	Yes	Fecal	H2 (29)
CC2	+	4	Yes	Sporadic	H10 (29)
CC2	+	5	Yes	Sporadic	H19 (29)
CC2	+	2	Yes	Fecal	H27 (29)
CC2	+	3	Yes	Epidemic	Scott A (29)
CC2	+	4	Yes	Food	2-9 (75)
CC2	+	5		Food	2-10 (75)
CC3		5	Yes	Fecal	H6 (29)
CC3		6	Yes	Sporadic	H7 (29)
CC3		3		Sporadic	H18 (29)
CC3		2	Yes	Fecal	H28 (29)
CC3		2		Fecal	H35 (29)
CC3		3	Yes	Food	2-13 (75)
CC3		3		Food	2-14 (75)
CC4	+	3	Yes	FPE	2-15 (75)
CC4	+	3		Food	2-16 (75)
CC5		2		Food	2-17 (75)
CC5		3	Yes	Food	2-18 (75)
CC6	+	3		Sporadic	H24 (29)
CC6	+	6	Yes	Food	2-19 (75)
CC6	+	4		Food	2-20 (75)
CC88		2		Sporadic	H9 (29)
CC220		2		Food	3-8 (75)
CC315		3		Food	3-14 (75)
Lineage II					
CC7		2	Yes	Sporadic	H3 (29)
CC7		2	Yes	Sporadic	H5 (29)
CC7		2		Sporadic	H13 (29)
CC7		2		Sporadic	H16 (29)
CC7		5		FPE	1-12 (75)
CC7		2	Yes	FPE	1-13 (75)
CC7		4		FPE	1-14 (75)
CC7		4		FPE	1-15 (75)
CC7		5		FPE	1-16 (75)
CC7		3		FPE	1-17 (75)
CC7		2		FPE	1-18 (75)
CC7		3		FPE	1-19 (75)
CC8		5	Yes	Fecal	H1 (29)
CC8		3		Sporadic	H15 (29)
CC8		2	Yes	Food	2-7 (75)
CC8		2		Food	2-8 (75)
CC9	−	3	Yes	Fecal	LO28 (29)
CC9	−	4	Yes	Epidemic	EGD-e (29)
CC9	−	2	Yes	Food	2-4 (75)
CC9	−	3		Food	2-5 (75)
CC9	−	2		Food	2-6 (75)
CC11		5		FPE	1-5 (75)
CC11		2	Yes	FPE	1-6 (75)
CC11		6		FPE	1-7 (75)
CC14		2		NA	3-2 (75)
CC18		2		Sporadic	H25 (29)
CC18		2	Yes	Fecal	H31 (29)
CC19		2		Food	3-4 (75)
CC20		2		Food	3-6 (75)
CC21		5	Yes	Sporadic	H8 (29)
CC21		3		Food	3-7 (75)
CC26		3		Food	3-9 (75)

(Continued on next page)

TABLE 1 (Continued)

Lineage[a] and MLST	Maury's classification[b]	LT50 (days)	RNA-seq[c]	Origin[d]	Isolate (reference)
CC26		2		Food	3-10 (75)
CC26		2	Yes	Food	3-11 (75)
CC31		2		Food	3-12 (75)
CC31		3		FPE	3-13 (75)
CC37		2		Fecal	H38 (29)
CC121	−	3	Yes	Fecal	H11 (29)
CC121	−	4	Yes	Fecal	H17 (29)
CC121	−	2	Yes	Fecal	H32 (29)
CC121	−	2		Fecal	H34 (29)
CC121	−	3		Food	1-1 (75)
CC121	−	6		Food	1-2 (75)
CC121	−	2	Yes	FPE	1-3 (75)
CC121	−	5		FPE	1-4 (75)
CC121	−	3		Food	2-1 (75)
CC121	−	3		Food	2-2 (75)
CC121	−	1		Food	2-3 (75)
CC155		6		FPE	1-8 (75)
CC155		3	Yes	FPE	1-9 (75)
CC155		6		FPE	1-10 (75)
CC155		6		Food	1-11 (75)
CC177		2		Food	3-3 (75)
CC199		2		Food	3-5 (75)
CC412		3		Food	3-15 (75)
CC451		2		Food	3-1 (75)
ST13		3	Yes	Food	3-18 (75)
ST13		6		Food	3-19 (75)
ST200		4	Yes	Food	3-16 (75)
Lineage NA[e]					
ST517		3		Food	3-17 (75)
NA		2		Sporadic	H23 (29)

[a]Lineage was determined based on the online MLST database for *L. monocytogenes* (http://bigsdb.pasteur.fr/listeria/).
[b]Maury's classification of genotypes (11) into hypervirulence (+) and hypovirulence (−).
[c]Isolates included in RNA-seq are noted as "Yes."
[d]FPE, food processing environment; NA, information not available.
[e]NA, information not available.

and "Detoxification"). In sum, PC1 represented transcriptome differences caused by the transition from exponential to early stationary phase.

PC2 explained 11.2% of the total variance, and other axes explained less than 10% fraction of variance. In total, 89.2% of variance was explained by 15 axes (Fig. 5A). Correlation analyses were performed to identify the contextual variables captured by the different PCs underlying heterogeneity. The coordinates of the two biological replicates (biological replicate 1 [BR1] and BR2) were more consistent for some PCs than for others as reflected in the variation of the Pearson correlation coefficient (r) computed between the vectors of 33 coordinates available for each biological replicate (Fig. 5B). In particular, coordinates on PC2 exhibited little correlation between the two biological replicates ($r = 0.17$), whereas the highest level of correlation was reached for PC3 ($r = 0.88$). Computation of Spearman's rank correlation coefficient (ρ) served as a generic approach to assess relationships between coordinates on each PC and ordinal (LT50 and Maury's classification) or binary (lineage and BR) covariates (Fig. 5C). Among the PCs, coordinates on PC3 and PC5 revealed the highest correlations with *in vivo* virulence (LT50) ($\rho = 0.26$ and $\rho = 0.33$, respectively). Concomitantly, Maury's classification of the genotypes exhibited positive correlations with PC1 ($\rho = 0.33$) and PC5 ($\rho = 0.39$), reflecting a trend of higher coordinates on these axes for samples corresponding to hypervirulent genotypes, and negative correlation with PC4 ($\rho = -0.47$). The exact opposite pattern was observed with respect to the division between lineages I and II: PC1 ($\rho = -0.31$) and PC5 ($\rho = -0.76$) exhibited negative correlations, reflecting

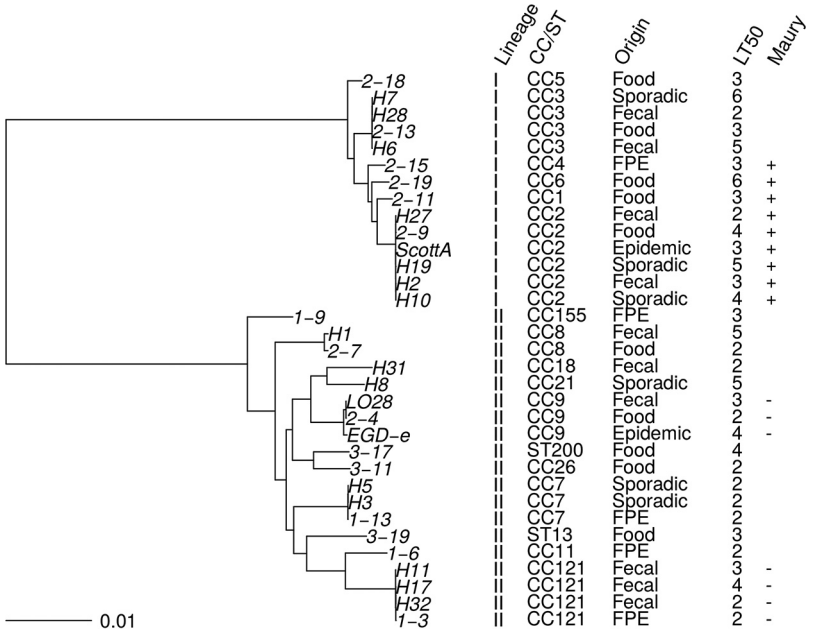

FIG 2 Phylogenetic tree reconstructed on the basis of whole-genome sequences for the 33 *L. monocytogenes* isolates selected for transcriptome profiling. The columns to the right of the phylogenetic tree show lineage, MLST genotype (clonal complex [CC] or sequence type [ST]), origin (FPE, food processing environment), virulence level expressed as LT50 (in days) measured in *G. mellonella*, and Maury's classification (11). Maury's classification (virulence-associated genotype) is shown as follows: +, hypervirulence; −, hypovirulence. Branch length represents the expected number of substitutions per base.

a trend of lower coordinates for samples corresponding to lineage II, whereas PC4 exhibited positive correlation ($\rho = 0.46$). This result was expected because of the aforementioned exclusive distribution of hyper- and hypovirulence genotypes in lineages I and II, respectively. Furthermore, in conjunction with the lower correlation between the coordinates of two biological replicates on PC2, it showed that PC2 tended to separate the two replicates ($\rho = 0.65$), with a trend of higher coordinates for samples corresponding to the BR2.

Dissimilarity between BRs was further investigated by analyzing the new transcriptome data sets generated by removing the variations captured by preceding PCs (Fig. 5D). The result revealed that jointly filtering out the variations captured by PC1 (reflecting transition of growth phases) and PC2 (reflecting a difference between the two BRs) globally decreased the distance between the two transcriptome profiles (BRs) available for each isolate.

(ii) Construction of a new data set with improved statistical power. Because large variations in transcriptome profiles related to transition of growth phase and systematic differences between BRs can mask more subtle variations associated with the characteristics of the isolates, a refined transcriptome data set was generated by filtering out variations captured by PC1 and PC2 from the original data set. Technically, this data set consisted of the residuals of the PCA projection on the subspace formed by PC1 and PC2. This processing step increased reproducibility of the transcriptome profiles between biological replicates (Fig. 6A) as predicted by the Pearson correlation analysis (Fig. 5D). We also confirmed that it significantly increased the statistical power of some correlation analyses between the transcript levels of individual genes and phenotypic values such as LT50 (Fig. 7). Namely, we examined the distribution of Spearman's rank correlation between each individual gene (*i*) and each of the three isolates characteristics (LT50, Maury's classification, and lineage number), denoted by *c*. This was done in terms of quantiles corresponding to the values of $\rho_{i,c}$ under the null hypothesis of no statistical association between transcript levels and covariate values such that departure from the uniform distribution is the landmark of the presence of

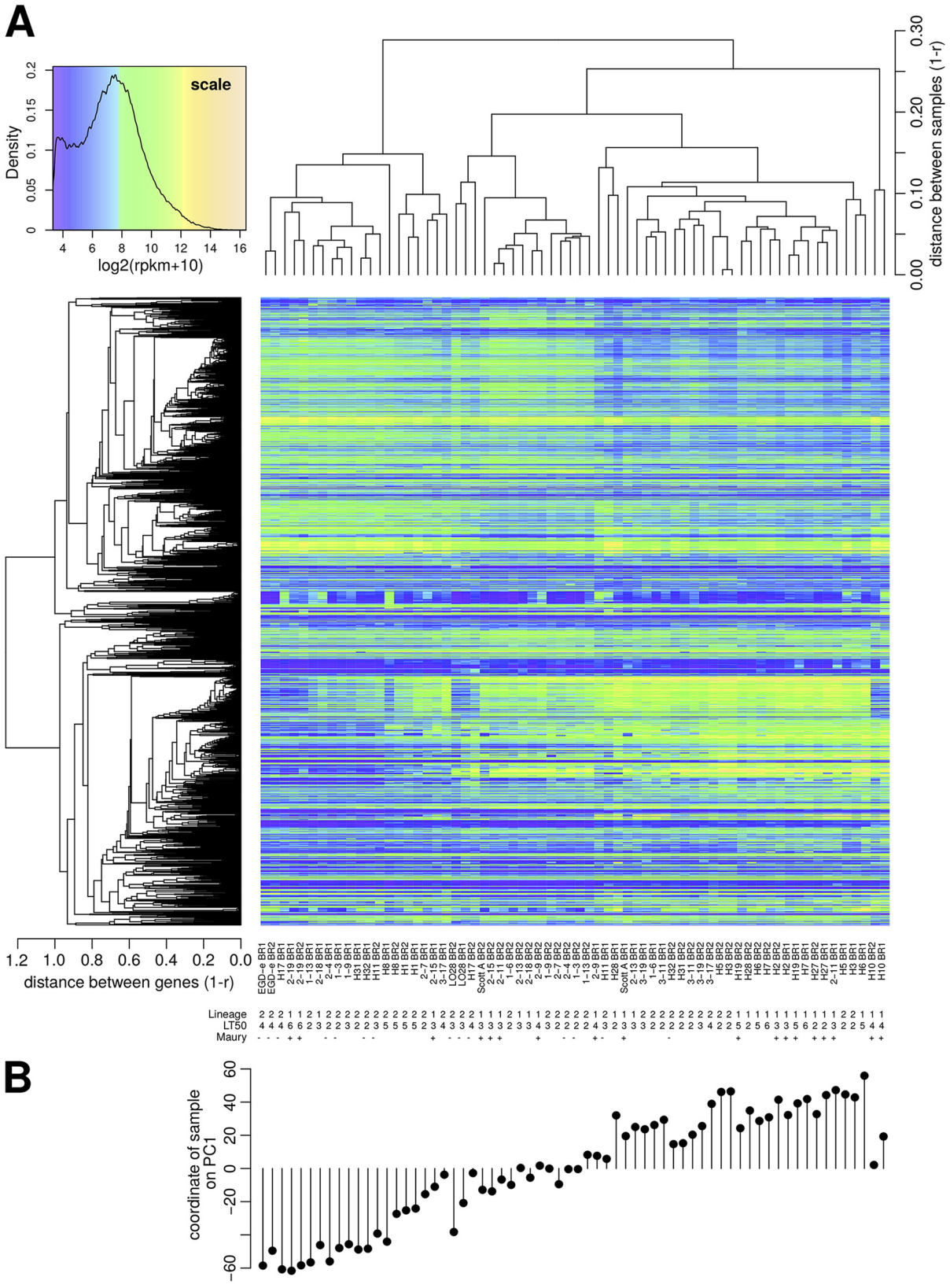

FIG 3 High variability in the original transcriptome data. (A) Heatmap representation of transcript levels (rpkm) expressed in $\log_2$ scale for 2,456 genes (row) and 66 samples (column). (B) Coordinates of samples on principal-component axis 1 (PC1), which accounts for 48.4% of the total variance, reveal a continuum of transcriptome profiles. For the purpose of this representation, coordinates on PC1 served to reorder the samples to highlight the continuum of transcription profiles. This reordering was made possible by the fact that many different orderings were consistent with the structure imposed by the dendrogram shown in the top part of the heatmap.

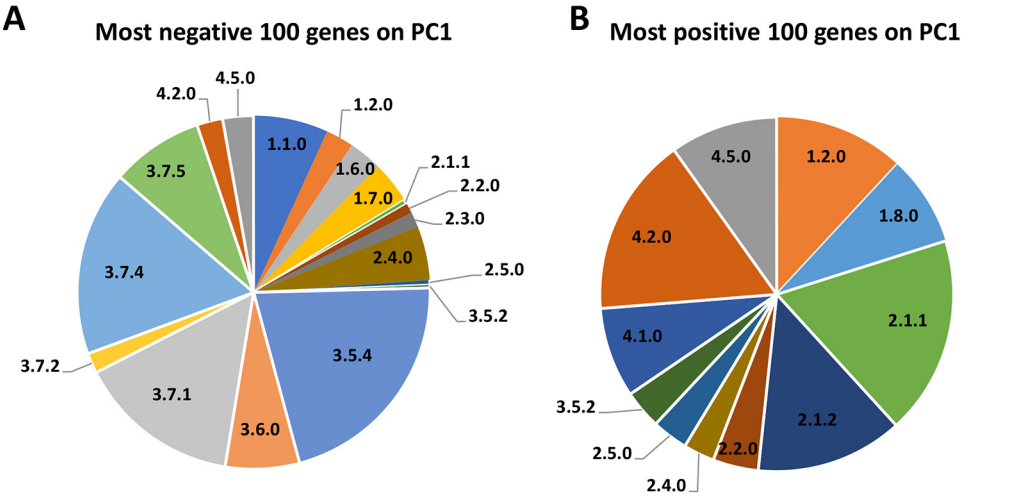

Code	Functional category description
1.1.0	Cell envelope and cellular processes > Cell wall
1.2.0	Cell envelope and cellular processes > Transport/binding proteins and lipoproteins
1.6.0	Cell envelope and cellular processes > Protein secretion
1.7.0	Cell envelope and cellular processes > Cell division
1.8.0	Cell envelope and cellular processes > Cell surface proteins
2.1.1	Intermediary metabolism > Metabolism of carbohydrates and related molecule > Specific pathways
2.1.2	Intermediary metabolism > Metabolism of carbohydrates and related molecule > Main glycolytic pathways
2.2.0	Intermediary metabolism > Metabolism of amino acids and related molecules
2.3.0	Intermediary metabolism > Metabolism of nucleotides and nucleic acids
2.4.0	Intermediary metabolism > Metabolism of lipids
2.5.0	Intermediary metabolism > Metabolism of coenzymes and prosthetic groups
3.5.2	Information pathways > RNA synthesis > Regulation
3.5.4	Information pathways > RNA synthesis > Termination
3.6.0	Information pathways > RNA modification
3.7.1	Information pathways > Protein synthesis > Ribosomal proteins
3.7.2	Information pathways > Protein synthesis > Aminoacyl-tRNA synthetases
3.7.4	Information pathways > Protein synthesis > Elongation
3.7.5	Information pathways > Protein synthesis > Termination
4.1.0	Other functions > Adaptation to atypical conditions
4.2.0	Other functions > Detoxification
4.5.0	Other functions > Miscellaneous

FIG 4 Principal-component axis 1 (PC1) distinguishes variations arising from changes in growth stage. Distribution of functional categories among genes that contribute most to PC1 is displayed in the pie chart. Genes of the 100 most negative loading values (A) and the 100 most positive loading values (B) were selected, and the relative ratio (number in 100 genes/number in whole genome) of each functional category was calculated. Categories corresponding to uncharacterized genes (i.e., "Similar to unknown proteins" and "No similarity") were excluded from the analysis.

statistically significant associations and can be directly used to estimate false-discovery rates as summarized in *q* values (45). While no statistical association between gene and LT50 was found with the original data (lowest *q* value, 0.18; Table S2), 25 genes were attributed *q* values below 0.10 based on the new data set. Not surprisingly given the correlation between PC1 (growth phase) and the two other characteristics (Maury's classification of genotypes and lineage number), filtering out the variations captured by PC1 and PC2 slightly decreased the number of statistically significant associations. However, we reasoned that statistical association between growth phase and Maury's classification (more advanced for hypervirulent genotypes) and lineage (less advanced for lineage II) could still be considered a confounding factor when pinpointing associations between these factors and individual genes, which also justifies working with the new data set. In sum, removing variations captured by PC1 and PC2 reduced protocol-driven noise and thereby increased statistical significance and biological relevance of correlations.

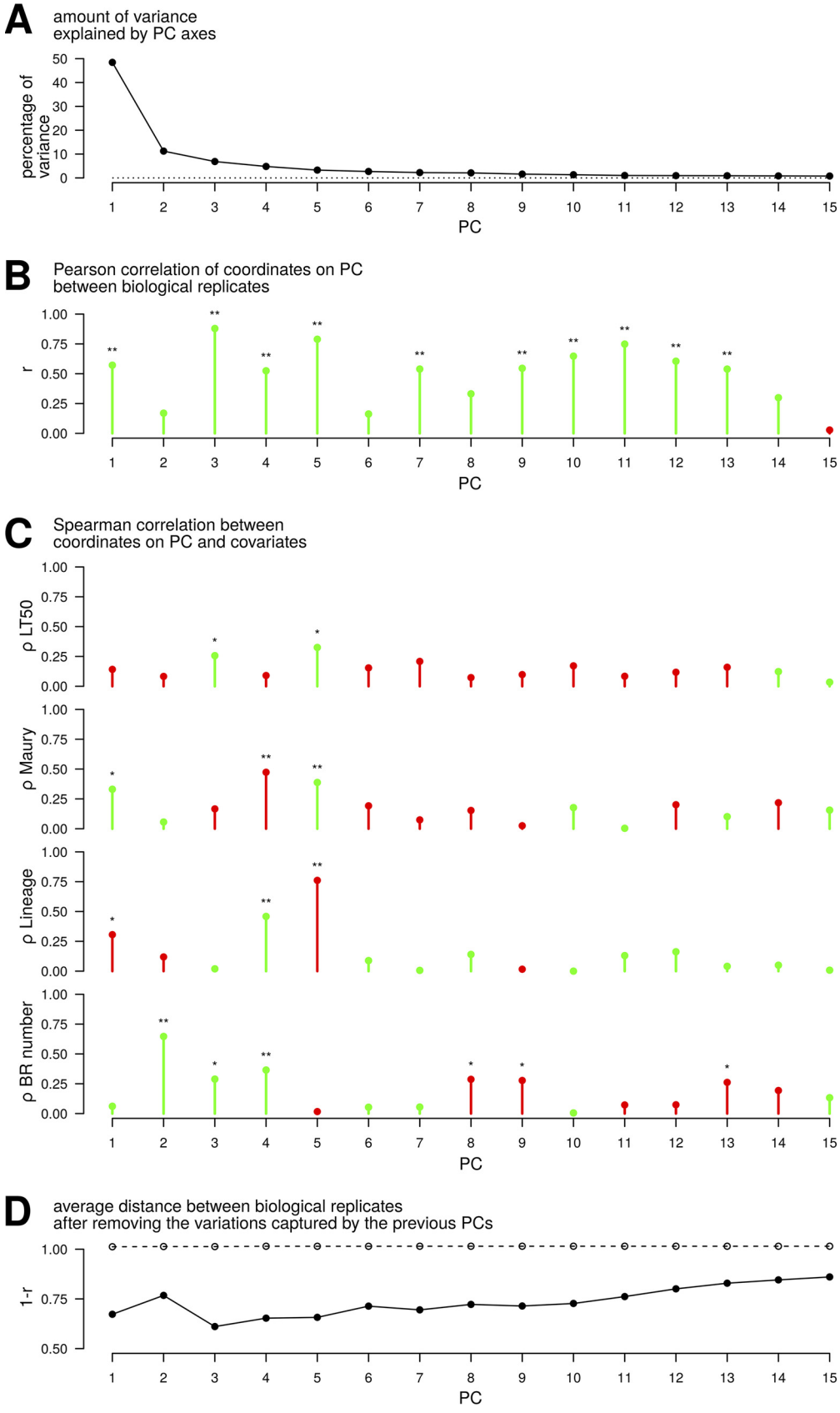

FIG 5 Principal-component axes (PCs) explain relationships between transcriptomes and variables. (A) Variance in transcriptomes captured by each PC is expressed as a percentage. The first two axes, PC1 and PC2, express 59.6% of

(Continued on next page)

(iii) Comparison to known regulons. Genes were clustered according to the similarity in expression patterns based on the refined data set (left dendrogram in Fig. 6A). Clusters of highly correlated genes (defined by average pairwise Pearson correlation greater than 0.6) were numbered according to their sizes. Summarizing for each gene the level of variability by the maximum $\log_2$ fold change between any pair of samples pinpointed 12 main clusters of genes with highly variable transcription levels (Fig. 6B and Table S3). Each of these clusters contained at least eight genes, half of which displayed a maximum $\log_2$ fold change higher than four. Taken together, they encompassed 11.5% (283 genes) of the core genome: 101 genes in cluster 1, 48 genes in cluster 3, 26 genes in cluster 4, and from 8 to 17 genes in the remaining clusters. The gene content of these 12 clusters were investigated in detail, since they reflected the main components of transcriptome plasticity. Clustered genes were compared to previous knowledge of the regulons of 32 transcription factors in order to scrutinize the regulatory networks. Regulons of 8 transcription factors, including the 4 sigma factors (46, 47), CtsR (48), CodY (49), VirR (50), and PrfA (51) were collected from the literature, and regulons of the 24 phylogenetically conserved transcription factors were retrieved from the RegPrecise database (52) (http://regprecise.lbl.gov/RegPrecise/genome.jsp?genome_id=210). Potentially σ^B-regulated genes accounted for 86% of cluster 1 and 88% of cluster 4, which is consistent with the proximity of the two clusters in the hierarchical clustering tree (left dendrogram in Fig. 6A). At a distance in the tree, clusters 30 and 45 also included 67% and 50% of genes previously linked to σ^B. In sum, eight clusters contained 41% (130 genes) of the core genome genes previously reported as probable members of the σ^B regulon. Clusters 14, 45, 3, and 30 were dispersed throughout the tree and included 54%, 50%, 35%, and 22%, respectively, of genes previously reported as regulated by CodY. Altogether, they accounted for 42% (30 genes) of the genes previously associated with CodY regulon. In cluster 26, 70% of the genes were probable members of the ArgR regulon which accounted for the whole list of genes linked to this transcription factor. Concurrently, six core PrfA virulons (*plcB*, *actA*, *mpl*, *hly*, *pclA*, and *inlC*) accounted for 75% of the genes of cluster 41 (51). Log_2 transcript levels of these core PrfA virulon genes are represented in Fig. S1 in the supplemental material. In total, taking into account other PrfA-regulated genes sparsely located in clusters 1, 4, and 7, 40% of the genes linked to PrfA were detected after clustering. Finally, 52 genes previously identified as virulence-related (40) were highlighted in the heatmap (Fig. 6A). Their dispersed position implies heterogeneous expression patterns among samples.

(iv) Correlation with phylogeny, CC-based virulence potential, and virulence phenotype. The refined data set was further exploited to delineate sets of genes whose transcript levels were correlated with lineage, Maury's classification, and experimental virulence phenotype (LT50). The number of genes whose expression levels were highly correlated ($|\rho| \geq 0.4$) with each of these characteristics was computed (Table 2).

A total of 473 and 222 genes correlated with lineage and Maury's classification, respectively (Tables S4 and S5). Among the 111 genes positively correlated with Maury's classification (higher transcript levels in more-virulent CCs), 77% overlapped in the set of 261 genes negatively correlated with lineages (higher transcript levels in lineage I). Similarly, 80% of the 111 genes negatively correlated with Maury's classification were present in the set of 212 genes positively correlated with lineage. As mentioned earlier, this high congruency is ascribable to the exclusive distribution of the hyper- and hypovirulent genotypes in lineages I and II, respectively. Only seven and

FIG 5 Legend (Continued)
total data set inertia. (B) Pearson correlation coefficient (r) is measured between coordinates of biological replicates (BRs) on each PC. (C) Spearman correlation coefficient (ρ) is measured between coordinates on each PC and the original covariates as follows: virulence measured in *G. mellonella* ("LT50"), genotypes related to hyper- or hypovirulence ("Maury"), phylogenetic division ("lineage"), and sets of BR ("BR number"). Green and red colors indicate positive and negative correlations, respectively. (D) After eliminating the variations captured by the previous PCs, the average distances between BR are calculated as "$1 - r$" (r is the Pearson correlation coefficient). For example, point PC3 on the x axis shows the average distance after removing variations captured by PC1 and PC2. *, $P \leq 0.05$; **, $P \leq 0.005$.

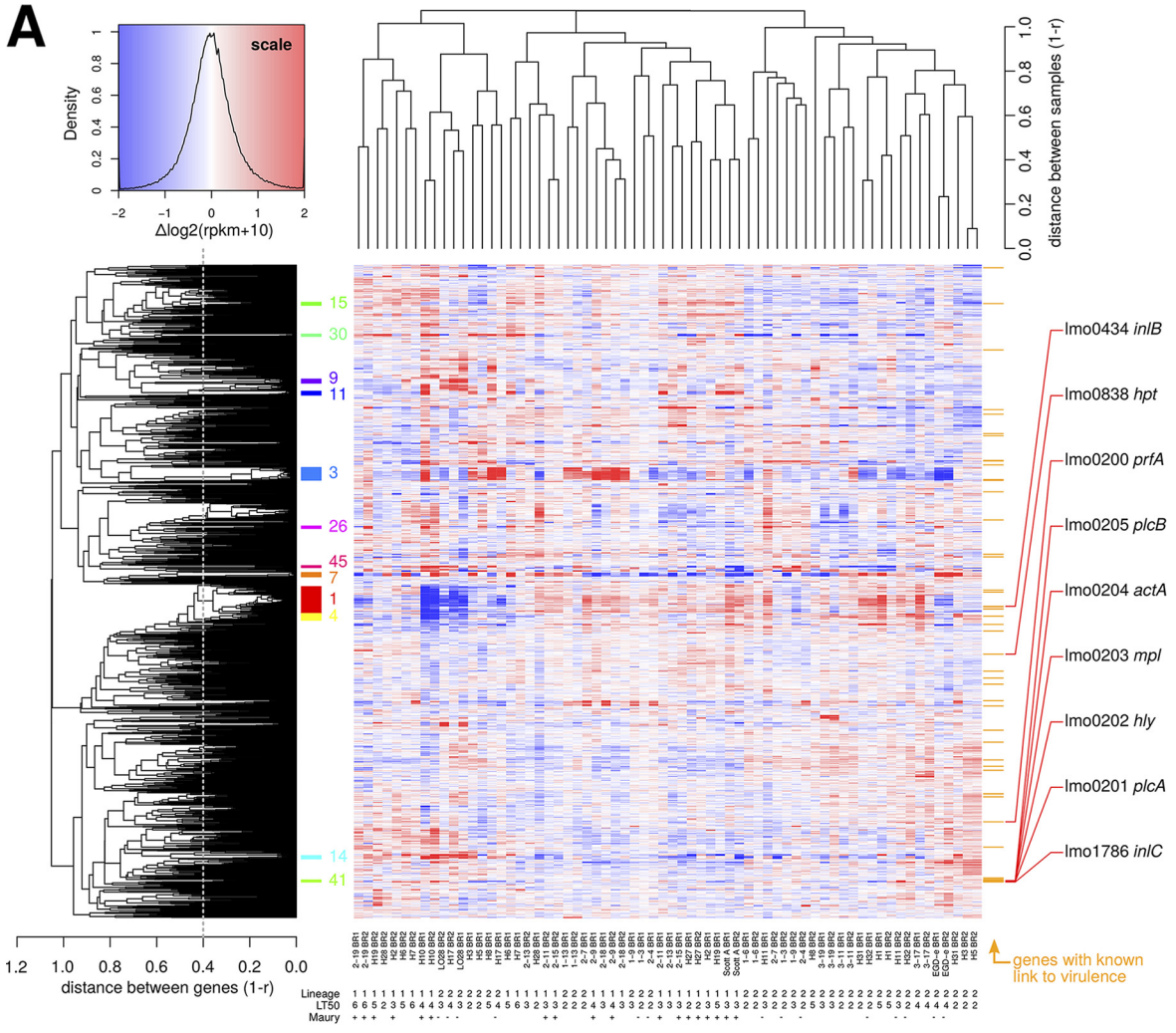

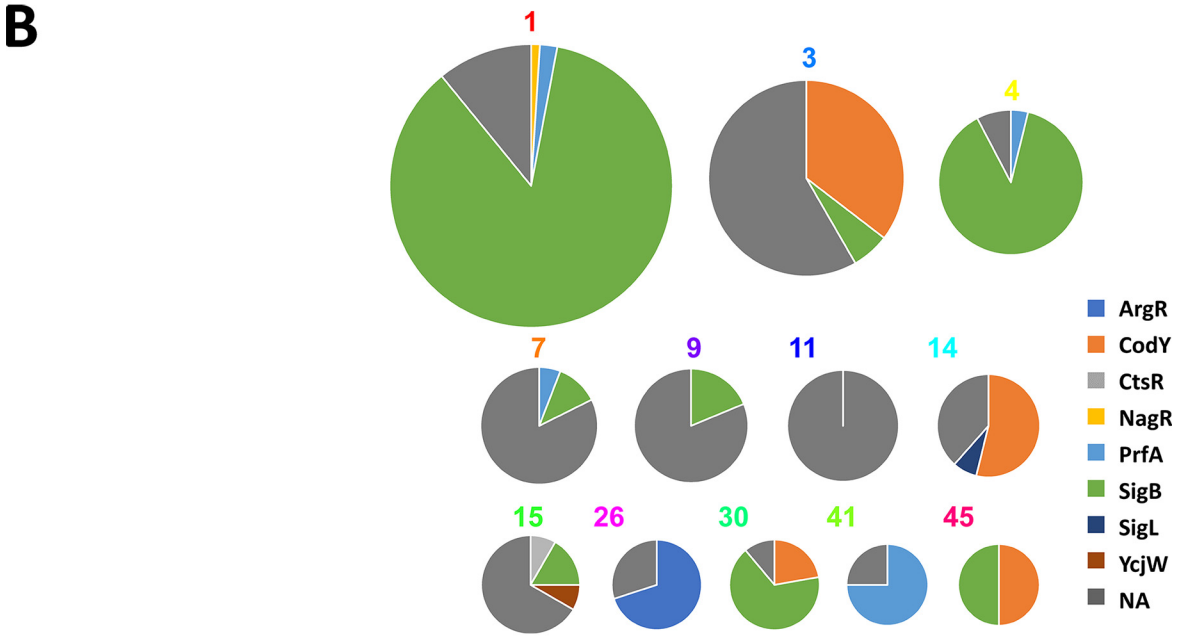

FIG 6 Analysis of the refined transcriptome data set created by filtering out the variations captured by PC1 and PC2. (A) Heatmap representing transcript levels (rpkm) in $\log_2$ scale expressed for 2,456 genes (rows) and 66 samples (columns). Cutoff at a Pearson correlation

(Continued on next page)

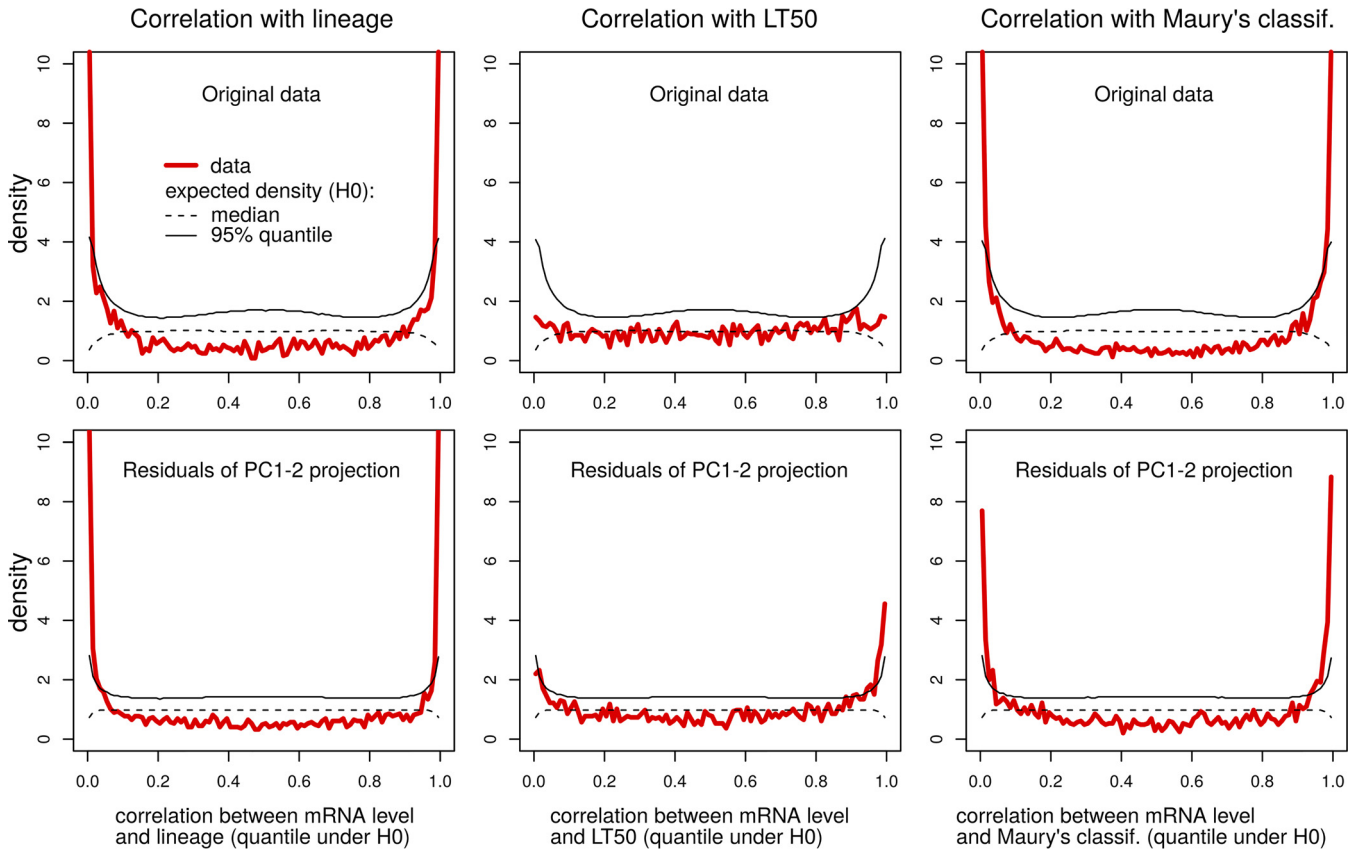

FIG 7 Impact of removing PC1 and PC2 on the correlation analysis between transcriptome profiles and isolate characteristics. For each correlation analysis, a plot shows the distribution of the Spearman correlation coefficients expressed in terms of quantile under the null hypothesis (H0) of no association (i.e., random permutations of the isolate labels) such that deviation from the uniform reflects statistical significance, values near 0 correspond to negative correlations, and values near 1 correspond to positive correlation. Distribution of the correlation coefficients for the actual data set (red line) is plotted along with the median (50% quantile, dashed black line) and the 95% quantile (black line). Distribution of quantiles for the adjusted data set (bottom row) reveals enhanced statistical power in Spearman correlation analysis compared to the original data set (top row).

three of the genes known to be linked with virulence in *L. monocytogenes* (40) were identified in the sets of lineage- and Maury's classification-associated genes, respectively. Heatmap representation of the transcription levels of the genes that were the most correlated to lineage and Maury's classification were able to discriminate the two lineages and to concurrently group together the isolates with similar virulence potential according to Maury's classification (Fig. 8A).

The sets of lineage- and Maury's classification-correlated genes were further examined in light of the functional categories (Fig. 9). Due to the overlap between lineage and Maury's classification of genotypes, the two correlation analyses tended to reveal similar enrichment patterns with respect to functional categories. Transcripts showing increased expression in lineage II ($\rho \geq 0.4$) were enriched (more than onefold) in the functional categories "Transformation/competence" and "DNA recombination." The categories "Sensors (signal transduction)," "Metabolism of phosphate," and "Detoxification" exhibited the same trend, albeit to a lesser extent. In contrast, transcripts showing increased expression in lineage I ($\rho \leq -0.4$) were enriched in the functional categories "Soluble internalin" and "RNA modification." Of note, the functional catego-

FIG 6 Legend (Continued)
coefficient of 0.6 identifies 12 clusters with more than 8 genes and fold change of ≥4. The clusters are indicated by colored bars with cluster identification numbers to the right of the dendrogram. Genes with known link to virulence (40) are shown by bars to the right of the heatmap, and core PrfA virulons (51) are indicated. (B) Relative abundance of regulons belonging to each cluster is expressed in the pie chart. The cluster number is marked above each circle, and the area of each circle is proportional to the number of genes composing the cluster. A complete list of the genes can be found in Table S3 in the supplemental material. NA, information not available.

TABLE 2 Comparison of the number of genes selected by Spearman correlation analysis with different variates (lineage, Maury's classification of genotypes, and *in vivo* virulence)

Characteristic	Value by parameter and correlation					
	Lineage[a]		Maury's classification[b]		LT50[c]	
	Negative	Positive	Negative	Positive	Negative	Positive
Designation	Lineage_N	Lineage_P	Maury_N	Maury_P	LT50_N	LT50_P
No. of genes[d]	261	212	111	111	17	39
Mean ρ	−0.54	0.55	−0.48	0.48	−0.44	0.45
FDR[e]	0.01	0.01	0.04	0.03	0.18	0.15
No. of shared genes						
Lineage_N	261	0	0	85	0	24
Lineage_P	0	212	89	0	13	0
Maury_N	0	89	111	0	11	0
Maury_P	85	0	0	111	0	9
LT50_N	0	13	11	0	17	0
LT50_P	24	0	0	9	0	39
Virulence genes[f]						
No. of genes	1	6	3	0	0	0
P value	0.04	0.45	0.50	0.17	1.00	1.00
Compared to Severino et al. (41)[g]						
481 (Lineage II > I)	33	71				
462 (Lineage I > II)	73	22				

[a]Lineage II versus lineage I in relation to transcript levels.
[b]Hyper- versus hypovirulent genotypes (11) in relation to transcript levels.
[c]Higher versus lower LT50 measured in *G. mellonella* in relation to transcript levels.
[d]Number of genes having a $|\rho|$ of ≥0.4 (ρ is the Spearman correlation coefficient).
[e]False-discovery rate (FDR) calculated by averaging the local FDRs.
[f]Compared to previously identified virulence-related genes (40).
[g]Compared to previously identified differentially expressed genes (41) available in our transcriptomes.

ries "Protein modification" and "Protein folding" were more than onefold enriched in both analyses; however, they were more highly enriched in genes with increased expression in lineage I. Additionally, hypervirulence ($\rho \geq 0.4$) was correlated with "Protein secretion," "Cell division," "Metabolism of lipids," "Metabolism of coenzymes and prosthetic groups," "Metabolism of phosphate," "DNA packaging and segregation," and "Similar to unknown proteins from *Listeria*." The categories "Metabolism of amino acids and related molecules" and "Protein folding" were associated with hypovirulence ($\rho \leq -0.4$).

(v) Transcripts whose expression is correlated with virulence level measured in *G. mellonella*. Because higher LT50 means lower virulence, negative ρ indicates positive correlation between *in vivo* virulence and transcript level. A total of 56 genes were identified ($|\rho| \geq 0.4$) of which 39 had a ρ of ≥0.4 and 17 had a ρ of ≤−0.4 (Fig. 8B). None of these genes (Table 3) were previously reported as directly virulence associated (40). A total of 14 genes belonged to the category "Cell envelope and cellular processes," 11 to "Intermediary metabolism," 3 to "Information pathways," and 2 to "Other functions." For 26 genes of unknown function ("Similar to unknown proteins" and "No similarity or information not available"), the online HHpred suite was used to search for possibly remote homology to known protein structures (53). Diverse functions were predicted such as carbohydrate transport and metabolism (*lmo0635*, *lmo0879*, and *lmo2832*), defense mechanisms (*lmo0375* and *lmo1963*), lipid metabolism (*lmo1862* and *lmo1863*), histidine triad protein (*lmo2216*), energy production (*lmo1050*), translation and posttranslational modification (*lmo2078* and *lmo2127*), and permease (*lmo0831*). In addition, the 56 genes were compared to the list of virulence genes from the PATRIC database (https://www.patricbrc.org/), and two potential virulence factor genes (i.e., *lmo0763*, encoding a serine/threonine phosphatase [54], and *lmo0540*, encoding a penicillin-binding protein [55]) were identified. The heatmap representation (Fig. 8B) roughly split the samples conforming to the PCA result which highlighted that lineages and LT50 were both correlated to PC5 (Fig. 5C).

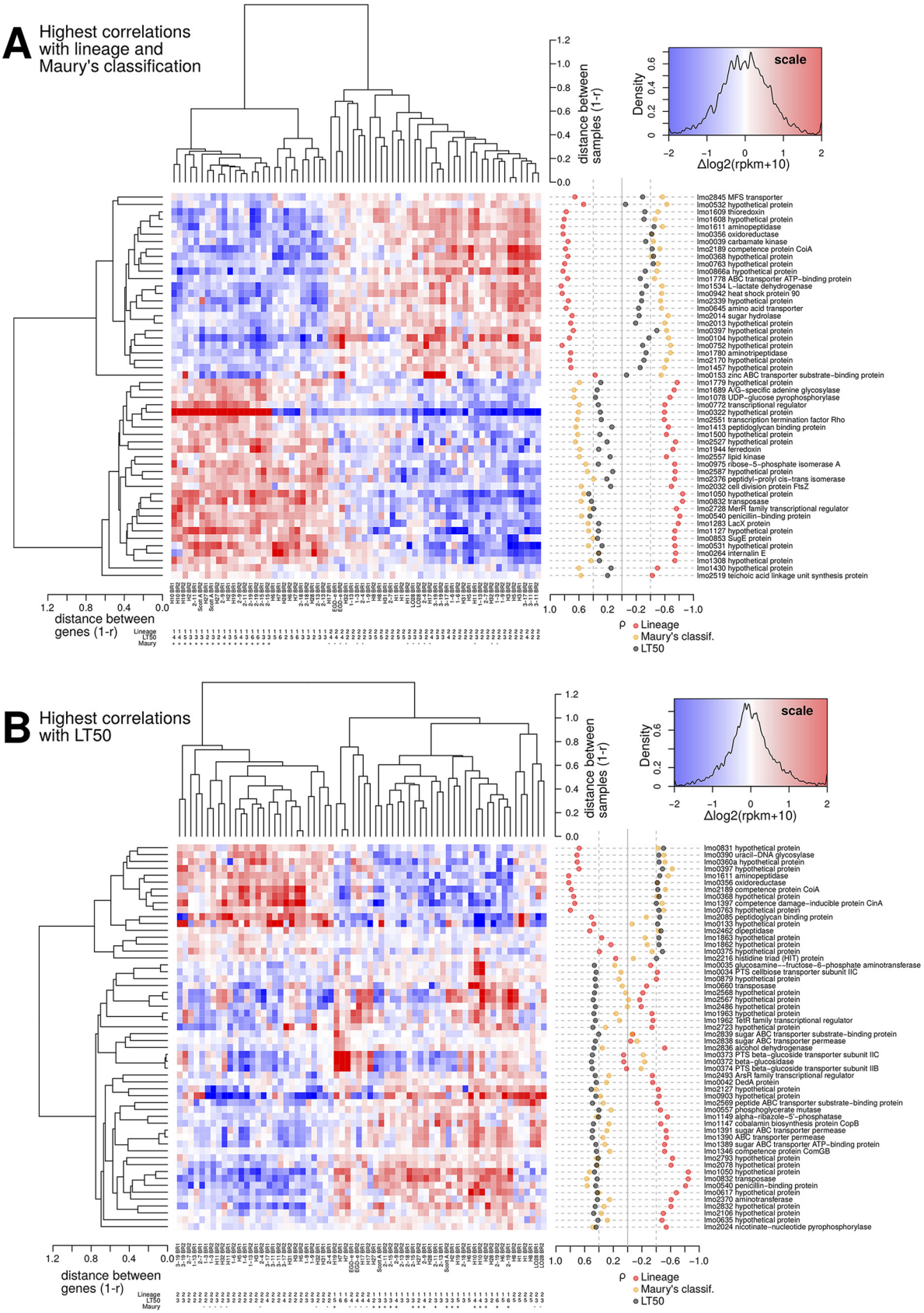

FIG 8 Highest correlation between transcript levels and covariates. (A) Transcripts corresponding to the 15 most extreme negative or positive ρ values with lineages (30 genes) and with Maury's classification of virulence genotypes (30 genes). Due to overlaps, the union between these

(Continued on next page)

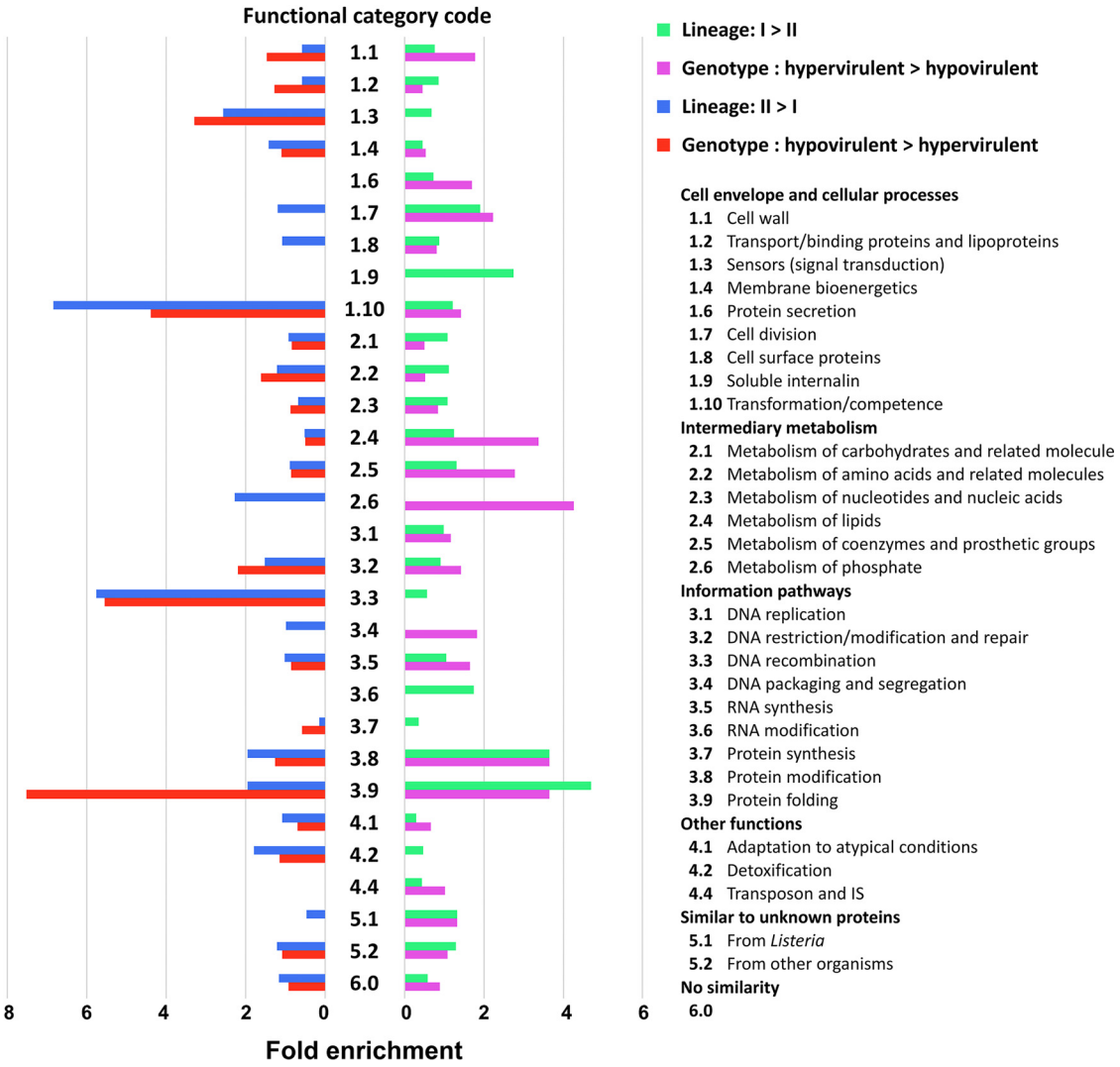

FIG 9 Functional classification of transcripts whose expression is correlated with division of lineages and Maury's classification. Among the lists of genes selected by Spearman's rank correlation analysis ($|\rho| \geq 0.4$), a total of 467 (99%) and 219 genes (99%) were designated to one of the categories, which is present in two higher hierarchies. Fold enrichment was calculated for each category as follows: fold enrichment = percentage in annotated genes/percentage in the whole genome of strain EGDe.

Among the 56 genes, three operon structures were identified based on the published operon map (17). Full operons 064 (*lmo0372*, *lmo0373*, and *lmo0374*) and 224 (*lmo1389*, *lmo1390*, and *lmo1391*) as well as two out of six genes in operon 330 (*lmo1858* to *lmo1863*) were found in the list. Moreover, among genes previously not identified in operon structure, four sets of genes at close loci displayed similar expression patterns across samples: *lmo0034* and *lmo0035*; *lmo1147* and *lmo1149*; *lmo2567* and *lmo2568*; *lmo2836*, *lmo2838*, and *lmo2839*.

DISCUSSION

Transcriptional reshaping is the cornerstone of the transition from saprophytism to infection (24). Interestingly, evidence suggests that assessment of *in vitro* basal tran-

FIG 8 Legend (Continued)
sets resulted in 52 genes. The figure combines a heatmap representation of transcript levels in $\log_2$ scale, with a graphical representation of the Spearman correlation coefficients with each covariate as semitransparent dots (red for lineage, orange for Maury's classification, and black for LT50 measured in *G. mellonella*). (B) Fifty-six transcripts corresponding to the highest correlations ($|\rho| \geq 0.4$) with virulence level determined in *G. mellonella* (LT50). Lists of the genes can be found in Table 3 and Tables S4 and S5 in the supplemental material.

TABLE 3 List of genes whose transcript levels are correlated with virulence measured in *G. mellonella*

Functional classification[a]	Locus tag	Spearman correlation analysis			Product	HHpred[d]
		Cor[c]	ρ value	*P* value		
1. Cell envelope and cellular processes						
Cell wall	*lmo0540*[b]	N	0.445	0.007	Penicillin-binding protein	
Cell envelope and cellular processes	*lmo0034*	N	0.438	0.003	Phosphotransferase system (PTS) cellobiose transporter subunit IIC	
	lmo0373	N	0.492	0.001	PTS beta-glucoside transporter subunit IIC	
	lmo0374	N	0.494	0.001	PTS beta-glucoside transporter subunit IIB	
	lmo1389	N	0.443	0.003	Sugar ABC transporter ATP-binding protein	
	lmo1390	N	0.494	0.001	ABC transporter permease	
	lmo1391	N	0.492	0.001	Sugar ABC transporter permease	
	lmo2569	N	0.491	0.001	Peptide ABC transporter substrate-binding protein	
	lmo2838	N	0.449	0.001	Sugar ABC transporter permease	
	lmo2839	N	0.404	0.002	Sugar ABC transporter substrate-binding protein	
Cell surface proteins	*lmo2085*	P	−0.448	0.006	Peptidoglycan binding protein	
Transformation/competence	*lmo1346*	N	0.433	0.001	ComGB; competence protein ComGB	
	lmo1397	P	−0.401	0.016	CinA; competence damage-inducible protein	
	lmo2189	P	−0.421	0.012	CoiA; competence protein	
2. Intermediary metabolism						
Metabolism of carbohydrates and related molecule	*lmo0035*	N	0.464	0.001	Glucosamine-fructose-6-phosphate aminotransferase	
	lmo0356	P	−0.416	0.013	Oxidoreductase	
	lmo0372	N	0.504	0.001	Beta-glucosidase	
	lmo0557	N	0.401	0.006	Phosphoglycerate mutase	
	lmo2836	N	0.469	0.000	Alcohol dehydrogenase	
Metabolism of amino acids and related molecules	*lmo1611*	P	−0.449	0.006	Aminopeptidase	
	lmo2370	N	0.421	0.006	Aminotransferase	
	lmo2462	P	−0.466	0.001	Dipeptidase	
Metabolism of coenzymes and prosthetic groups	*lmo1147*	N	0.477	0.001	CopB; cobalamin biosynthesis protein	
	lmo1149	N	0.405	0.005	Alpha-ribazole-5′-phosphatase	
	lmo2024	N	0.440	0.002	NadC; nicotinate-nucleotide pyrophosphorylase	
3. Information pathways						
DNA restriction/modification and repair	*lmo0390*	P	−0.436	0.004	Uracil-DNA glycosylase	
RNA synthesis	*lmo1962*	N	0.449	0.002	TetR family transcriptional regulator	
	lmo2493	N	0.452	0.001	ArsR family transcriptional regulator	
4. Other functions						
Transposon and IS	*lmo0660*	N	0.444	0.000	Transposase	
	lmo0832	N	0.425	0.010	Transposase	
5. Similar to unknown proteins						
From *Listeria*	*lmo0617*	N	0.423	0.007	Hypothetical protein	[PF16729.5_99.2%] DUF5067; domain of unknown function
	lmo2568	N	0.462	0.000	Hypothetical protein	[COG5294_99.9%] YxeA; uncharacterized protein YxeA, DUF1093 family (Function unknown)
From other organisms	*lmo0042*	N	0.437	0.001	DedA protein; uncharacterized membrane protein	[COG0586_99.8%] DedA; uncharacterized membrane protein DedA, SNARE-associated domain (Function unknown)
	lmo0133	P	−0.419	0.009	Hypothetical protein	[COG3592_98.2%] YjdI; uncharacterized Fe-S cluster protein YjdI (Function unknown)
	lmo0397	P	−0.488	0.003	Hypothetical protein	[cd08899_99.8%] SRPBCC_CalC_Aha1-like_6; putative hydrophobic ligand-binding SRPBCC domain of an uncharacterized subgroup of CalC- and Aha1-like proteins
	lmo0635	N	0.414	0.003	Hypothetical protein	[COG0637_99.9%] YcjU; beta-phosphoglucomutase or related phosphatase, HAD superfamily (Carbohydrate transport and metabolism, General function prediction only)
	lmo0763[b]	P	−0.438	0.007	Ser/Thr protein phosphatase family protein	[COG1408_100%] YaeI; predicted phosphohydrolase, MPP superfamily (General function prediction only)
	lmo0831	P	−0.502	0.001	Hypothetical protein	[COG0679_100%] YfdV; predicted permease (General function prediction only)
	lmo0879	N	0.453	0.003	Hypothetical protein	[COG3623_100%] SgaU; L-ribulose-5-phosphate 3-epimerase UlaE (Carbohydrate transport and metabolism)

(Continued on next page)

TABLE 3 (Continued)

Functional classification[a]	Locus tag	Spearman correlation analysis			Product	HHpred[d]
		Cor[c]	ρ value	*P* value		
	lmo0903	N	0.443	0.005	Hypothetical protein	[COG1765_99.9%] YhfA; uncharacterized OsmC-related protein (General function prediction only)
	lmo1050	N	0.463	0.006	Hypothetical protein	[COG1853_100%] RutF; NADH-FMN oxidoreductase RutF, flavin reductase (DIM6/NTAB) family (Energy production and conversion)
	lmo1862	P	−0.438	0.001	Hypothetical protein	[cd04506_99.9%] SGNH_hydrolase_YpmR_like; members of the SGNH-hydrolase superfamily, a diverse family of lipases and esterases
	lmo1863	P	−0.437	0.003	Hypothetical protein	[COG1307_100%] DegV; fatty acid-binding protein DegV (Lipid transport and metabolism)
	lmo1963	N	0.471	0.001	Hypothetical protein	[COG4200_99.6%] EfiE; predicted lantabiotic-exporting membrane pepmease, EfiE/EfiG/ABC2 family (Defense mechanisms)
	lmo2078	N	0.432	0.004	Hypothetical protein	[COG0802_100%] TsaE; tRNA A37 threonylcarbamoyladenosine biosynthesis protein TsaE (Translation, ribosomal structure and biogenesis)
	lmo2106	N	0.474	0.000	Hypothetical protein	[COG1408_100%] YaeI; Predicted phosphohydrolase, MPP superfamily (General function prediction only)
	lmo2127	N	0.507	0.001	Hypothetical protein	[COG1266_98.9%] YdiL; membrane protease YdiL, CAAX protease family (Posttranslational modification, protein turnover, chaperones)
	lmo2216	P	−0.403	0.000	Histidine triad (HIT) protein	[COG0537_99.9%] hit; diadenosine tetraphosphate (Ap4A) hydrolase or other HIT family hydrolase (Nucleotide transport and metabolism, Carbohydrate transport and metabolism, General function prediction only)
	lmo2486	N	0.450	0.000	Hypothetical protein	[PF13349.6_99.9%] DUF4097; putative adhesin
	lmo2723	N	0.484	0.002	Hypothetical protein	[COG2153_99.8%] ElaA; predicted *N*-acyltransferase, GNAT family (General function prediction only)
	lmo2832	N	0.452	0.004	Hypothetical protein	[COG1929_100%] GlxK; glycerate kinase (Carbohydrate transport and metabolism)
6. No similarity or no information available	*lmo0375*	P	−0.487	0.003	Hypothetical protein	[COG3077_90.9%] RelB; antitoxin component of the RelBE or YafQ-DinJ toxin-antitoxin module (Defense mechanisms)
	lmo2567	N	0.480	0.000	Hypothetical protein	[PF13314.6_86.3%] DUF4083; domain of unknown function
	lmo2793	N	0.411	0.005	Hypothetical protein	[PF17178.4_80.5%] MASE5; membrane-associated sensor
	lmo0360a	P	−0.438	0.005	Hypothetical protein	[PF14143.6_78.3%] YrhC; YrhC-like protein (Function unknown)
	lmo0368	P	−0.441	0.008	Hypothetical protein	[KOG0142_99.8%] isopentenyl pyrophosphate: dimethylallyl pyrophosphate isomerase (Secondary metabolites biosynthesis, transport and catabolism)

[a]Functional classification for *L. monocytogenes* EGDe (http://genolist.pasteur.fr/ListiList/).
[b]Virulence factors identified from PATRIC (https://www.patricbrc.org/).
[c]Correlation with virulence measured in *G. mellonella*. N, negative correlation; P, positive correlation.
[d]Homology detected by HHPred is expressed as: [identifier_probability percentage] product (function).

scription of some bacterial pathogens could be informative of their virulence level. For example, transcriptional profiling of methicillin-resistant and -susceptible cultures of *Staphylococcus pseudintermedius* identified differentially expressed genes such as surface proteins, toxins, and prophage genes that might contribute to virulence (42). In the current study, we produced a comprehensive transcriptome data set from which basal transcription patterns were analyzed in multiple aspects putatively associated with virulence potential. The experimental design of the current study specifically aimed at establishing links between phenotype and transcriptome across the diversity of the *Listeria monocytogenes* species. To optimize the statistical and biological relevance of the correlations with fixed resources, we maximized the number and diversity of

isolates profiled in the transcriptomic study by including only two biological replicates per isolate. These two biological replicates allowed us to assess the overall variability of the transcriptome profiles but imposed a limit on the power of pairwise comparisons of transcriptome profiles between genotypes, which is a question not directly linked to the identification of relations between transcriptome and phenotype. The study thus focused on correlation between transcriptome and phenotypes measured *in vivo* (in *G. mellonella*) or inferred from epidemiological data (Maury's classification). Given existing links between epidemiological data and lineages and to better understand the global pattern of variations in transcriptome profiles across isolates, correlation between transcriptome and lineage was also evaluated.

Exponentially grown cells in BHI at 37°C were used for transcriptomic analysis, since this *in vitro* condition was reported to be the closest to that of *L. monocytogenes in vivo* (36). Part of the core transcriptome variations was explained by slight differences in growth stage at the time of cell harvest. This variation was captured by PC1 that discriminated samples according to the transition from exponential to early stationary phase. Functional analysis revealed that while transcript levels of genes involved in protein synthesis reflected exponential phase, those involved in carbohydrate metabolism could be linked to the transition to early stationary phase. Indeed, a switch from glycolysis to gluconeogenesis is the most important metabolic rearrangement at the end of exponential growth in various organisms (56). Further systematic experimental noise between BRs was captured by PC2. Exclusion of these variations improved correlations and increased robustness of the conclusions drawn between transcript levels and covariates. Even though PC1 showed significant correlations with some covariates (Maury's classification and lineage), the improved statistical power of correlation analyses supported the rationale for using the new data set. This approach of using PCA to filter noise is reminiscent of its well-established use in genome-wide association studies to search for disease markers. In this context, PCA serves to overcome potentially confounding effects of population stratification from geographical attributes by allowing us to adjust genotypes and phenotypes using the main axes of variations (57, 58).

The statistical treatment unveiled significant correlations between large sets of genes with phylogenetic divergence. Among the most prominent differences in functional analysis, "Transformation/competence" and "DNA recombination" were overrepresented in lineage II isolates. It supports the current evolutionary history of *L. monocytogenes* characterized by higher recombination potential in lineage II than lineage I isolates which may have promoted successful adaptation of lineage II isolates to diverse environments (8). In contrast, functions related to pathogenicity were overrepresented in lineage I isolates. For instance, "Soluble internalin" was enriched only in lineage I, and functions related to posttranslational modifications, namely, "Protein modification" and "Protein folding," were more enriched in isolates of lineage I than in those of lineage II by 1.7- and 2.8-fold, respectively. Posttranslational modification is one of the crucial strategies employed by pathogens to modify the activity of virulence factors as well as to modulate host cell pathways to their benefit (59). A previous study using a macroarray compared the transcriptomes of six isolates (two lineage II isolates and four lineage I isolates) during late-exponential growth in defined medium supplemented with 1% glucose (41). The lack of overlap with the genes identified in the present study may be ascribed to differences in the experimental design and in statistical approaches. Technical variations in obtaining the expression values may have also contributed to the differences. Indeed, the current study used RNA-seq, while the previous study relied on a noisier technology. Moreover, investigating a larger collection of isolates allowed us to better capture intraspecific diversity here.

In spite of the high congruence between the set of transcripts correlated with lineage and Maury's classification of genotypes, functional analyses highlighted some differences. Genotype-specific features were mainly found in intermediary metabolisms: while "Metabolism of lipids," "Metabolism of coenzymes and prosthetic groups," and "Metabolism of phosphate" were highly enriched in CC1, CC2, CC4, and CC6,

"Metabolism of amino acids and related molecules" was highly enriched in CC121 and CC9. It is tempting to suggest that these differences in basal metabolism may be linked to niche-specific adaptation strategies which led to the current distribution of these CCs from clinical and environmental sources.

In our data, isolates were clustered according to genes sharing similar transcription patterns. Interestingly, 64% of these clustered genes were found to belong to published lists of regulons, among which were the core PrfA virulon. Considering that the published lists that we analyzed accounted for only 26% of the genes of *L. monocytogenes* EGDe, our clustering reflects the strong contribution of the known transcription factors to variability of gene expression during optimal growth.

The conserved innate immune response to microbial infections between insects and mammals as well as its cost efficiency and comparably fewer ethical concerns than with mammals makes *G. mellonella* an attractive *in vivo* model for evaluating virulence in bacteria (60), and it was successfully applied to *L. monocytogenes* (61, 62). In the present study, cells were synchronized to stationary phase during which bacterial physiology remains stable for a wider window of time so as to minimize undesired variations between assays and isolates. We reasoned that the initial growth phase is likely to have little weight on *in vivo* results, since cells washed with phosphate-buffered saline (PBS) and transferred to larval hemocoel experience physiological changes, including adaptation to the new environment before resuming infection. Certainly, bacterial adaptability to hemolymph and ability to hijack larval pathways for proliferation are one of the factors driving different levels of pathogenicity (63).

Spearman correlation analysis identified 56 genes whose transcript levels were positively or negatively correlated with *G. mellonella in vivo* virulence. None of the obvious virulence factors were represented among these genes, confirming that baseline expression of virulence genes strictly restricted to host cell invasion are poor markers of virulence potential. Among the correlated genes were phosphatases that broadly modulate activity of pathogenic bacteria and promote their intracellular growth (64). Similarly, lipid metabolism is important for intracellular life cycle, for example, to make use of host lipids as energy sources and to modulate host immune responses (65). Recent studies found existence of several type II toxin-antitoxin systems in *L. monocytogenes* connected to stress conditions (66, 67), though their role in virulence needs further investigation. Two competence genes (*lmo2189* and *lmo1397*) were positively correlated, while one (*lmo1346*) was negatively correlated to virulence level. The Com system of *L. monocytogenes* is required to promote escape from phagosomes during infection (68). The exact role of these competence proteins in virulence requires in-depth exploration. One of the negatively correlated genes was *lmo0540*, which encodes a penicillin-binding protein. Although disruption of *lmo0540* did not alter resistance to penicillin G and cephalosporins, an insertion mutant showed virulence attenuation *in vivo* (55). In contrast, other penicillin-binding proteins were reported to induce attenuation of virulence in some bacterial pathogens (69–71), even though antibiotic resistance is evolutionarily intertwined with bacterial virulence. Likewise, negative correlations between transcript levels of *lmo0540* and *lmo1963* (hypothetical lantibiotic-exporting membrane permease) and virulence in *G. mellonella* may suggest complex relationships between virulence and drug resistance. Other transcripts negatively correlated with virulence included genes involved in sugar transport (*lmo0034*, *lmo0373*, *lmo0374*, *lmo1389*, *lmo1390*, *lmo1391*, *lmo2838*, and *lmo2839*) and metabolism (*lmo0035*, *lmo0372*, *lmo0557*, *lmo2836*, *lmo0635*, *lmo0879*, and *lmo2832*). PrfA-mediated repression of virulence gene expression by specific carbohydrates is one of the subtle mechanisms that control the onset of infection (72, 73). Correspondingly, PrfA overexpression interferes with glucose uptake which resulted in impaired growth (74). In this regard, the current study showing lower basal transcript levels of those genes in more-virulent isolates grown in nutrient-rich BHI medium suggests further connections between central metabolism and infection. Detailed investigations of bacterial metabolism during infection must be assessed to explore possible links between bacterial fitness and virulence potential.

As a whole, our data evidenced vast variations in virulence phenotype and transcriptome profiles. PCA successfully filtered noise from the RNA-seq data set and strengthened experimental reproducibility. Clustering of several regulons across samples featured the role of key transcription factors such as σB, PrfA, and CodY in the observed transcriptome diversity. The phylogenetic position appeared to be a major factor underlying transcriptome diversity, since as much as 19% of the genes differentially transcribed correlated with lineage. This result documents a genome-wide physiological differentiation during evolution that parallels previously reported epidemiological differences. Although correlations between virulence determined in *G. mellonella* and transcriptomes were evidenced, it is challenging to identify molecular markers whose transcript levels could predict virulence. We hope that the present study can help in the design of future analyses, at an even more ambitious scale, that are needed to tackle the challenges of integrating epidemiological or experimental data on virulence with transcriptome data. Despite the high interest for this idea, it remains unclear at this stage whether transcriptomics could become useful as a predictive tool for virulence that could be applied to large collections of isolates.

MATERIALS AND METHODS

Isolate collection and culture condition. A collection of 91 *Listeria monocytogenes* isolates from various origins, serogroups, and genotypes was used in the current study (Table 1) (29, 75). These 91 isolates were of human origin (33 isolates) and food-related origin (58 isolates). Each experiment was performed with freshly prepared cultures from a stock kept at −80°C in brain heart infusion (BHI) broth (AES Laboratoire, France) with 8.5% glycerol (Sigma-Aldrich, France). After overnight incubation on BHI agar (AES Laboratoire) at 37°C, a few colonies were suspended in BHI broth and grown overnight at 37°C without aeration. Consecutive subculture (16 h, 37°C) was performed to prepare stationary-phase cells (mother culture) for infection. The cells were centrifuged (5,000 × *g*, 5 min, room temperature), and pellets were washed twice with phosphate-buffered saline (PBS). Washed cells were suspended in PBS and calibrated to obtain an optical density at 600 nm of 0.1. Part of the suspension was used for enumeration by serial dilutions in PBS and plating onto BHI agar to retrospectively determine the bacterial counts used for injection. CFU were counted after overnight incubation at 37°C.

Whole-genome sequencing and phylogenetic analysis. The genomes of 15 isolates had been sequenced in a previous study (75). The paired-end reads used in the study are available under the ENA bioprojects as follows: PRJEB15592 (https://www.ebi.ac.uk/ena/data/view/PRJEB15592) and PRJEB32254 (http://www.ebi.ac.uk/ena/data/view/PRJEB32254).

We sequenced additional isolates for phylogenetic analysis. Exponential cells were harvested by centrifugation at 5,000 × *g* for 10 min and washed twice with TE buffer (10 mM Tris-HCl [pH 7.5], 1 mM EDTA). Pelleted cells were resuspended in TE buffer, and cells were sonicated for 56 cycles (with one cycle consisting of 30 s on and 30 s off) at low frequency at 4°C using Bioruptor (Diagenode, Belgium) with several spin-downs at intervals. Fragmented genomic DNA was purified using Nucleospin PCR cleanup kit (Macherey-Nagel, Germany) and checked for quality and size using a Labchip GX II bioanalyzer. End repair was performed, followed by ligation of adapters (Illumina, USA), and the final product was purified using MagSi-NGSPrep Plus (AmsBio, UK). The concentration of each library was measured using Qubit dsDNA HS Assay (Thermo Fisher Scientific, France), and pooled libraries were subjected to additional purification using MagSi-NGSPrep Plus. Sequencing was conducted on Illumina NextSeq 500 platform (single-end, 1 × 75 bp per read). After quality control and trimming, *de novo* gene assembly was performed using SPAdes (76) for each genome library. The raw reads are available under the ENA bioproject PRJEB32882 (http://www.ebi.ac.uk/ena/data/view/PRJEB32882).

The 2,867 coding sequences (CDSs) annotated in *L. monocytogenes* EGDe (GenBank accession no. NC_003210; length, 2,944,528 bp) were mapped on the 33 assembled genomes to retrieve their pattern of presence/absence as well as all allelic variants. For this purpose, we used "tblastn" version 2.6.0+ with options "-task tblastn -evalue 1e-10 -seg no" (77) and cutoffs corresponding to 80% identity at the amino acid sequence and minimum coverage of 80% of the query. This procedure identified a total of 2,456 conserved single-copy genes whose amino acid sequences were subjected to separate multiple sequence alignments using MUSCLE version 3.8.31 with default parameters (78). Custom Perl scripts were used for conversion to nucleotide sequences, concatenation, and gap removing. The resulting alignment of 2,241,553 bp containing 167,253 single nucleotide polymorphisms (SNPs) served for phylogenetic tree reconstruction using PhyML version 20120412 with default parameters (79).

***Galleria mellonella* injection and virulence assay.** *Galleria mellonella* larvae in their final instar stage were used (Sud Est Appats Sarl, France). Each larva was injected with 10 μl (approximately 1.53 × 10^6 CFU) of stationary growing cells directly into the larval hemocoel via the last left proleg using ultrafine (29-gauge) needle insulin syringes. Ten larvae were injected per isolate. After injection, larvae were incubated at 37°C and monitored for survival at daily intervals postinfection up to day 5. Larvae showing no movement in response to external stimuli such as shaking of the petri dish and touching with a pipette tip were considered dead, and the time necessary to kill more than or equal to 50% of larvae (LT50) was recorded. Every trial included 10 larvae injected with PBS as a negative control in order

to confirm their viability. Any experiment which resulted in more than 20% mortality in control larvae was excluded. Assays were repeated at least three times.

RNA extraction and DNase I treatment. Mother cultures (see above) were inoculated into fresh BHI broth and grown at 37°C for 5 to 6 h to reach exponential phase. RNAprotect (Qiagen, USA) was added, and cultures were vortexed followed by incubation at room temperature for 5 min. The mixtures were pelleted by centrifugation (5,000 × *g*, 10 min, room temperature), and pellets were suspended in 5 M guanidine thiocyanate (Roth, Germany) lysis buffer with 10 μl/ml 2-mercaptoethanol (Sigma-Aldrich). To lyse cell walls, 0.5-mm glass beads (Roth) were added, and bacterial cells were homogenized using Tissulyser (Qiagen) at a frequency of 30 Hz for 6 min. After centrifugation (16,000 × *g*, 30 s, room temperature) supernatants were collected, and RNA was purified using column-based RNA Clean & Concentrator-5 kit (Zymo Research, Germany). The quality of extracted RNA was assessed using a Labchip GX II bioanalyzer (Perkin Elmer, USA). To remove DNA contamination, total RNA was incubated with Baseline-Zero DNase (Epicentre, France) in the presence of RiboLock RNase inhibitor (40 U/μl) (Thermo Fisher Scientific, Germany) for 30 min at 37°C, followed by purification using RNA Clean & Concentrator-5 kit. RNA concentration was measured using Qubit RNA HS Assay (Thermo Fisher Scientific).

Library preparation and sequencing. To enrich mRNA and remove rRNA, total RNA was treated by using a Ribo-Zero rRNA removal kit (Illumina). Briefly, beads were washed twice and hybridized with probes at 68°C for 10 min. Five hundred nanograms of total RNA was added to the mixture and incubated at room temperature and 50°C for 5 min each. rRNA bound to the beads was separated from mRNA using a magnetic stand. Enriched mRNA was then purified by using a RNA Clean & Concentrator-5 kit, and rRNA depletion was confirmed on the Labchip GX II bioanalyzer (Perkin Elmer).

Preparation of cDNA fragment libraries was performed using NEBNext Ultra II Directional RNA Library Prep kit for Illumina (Illumina) with slight modifications. Briefly, the enriched mRNA was fragmented for 15 min at 94°C and reverse transcribed to synthesize the first-strand cDNA followed by second-strand cDNA synthesis. Double-stranded cDNA (ds cDNA) was purified using NucleoMag (Macherey-Nagel) SPRI selection. End repair was performed on the ds cDNA library, followed by ligation of adapters. High-fidelity PCR was performed using KAPA Hifi polymerase (Kapa Biosystems, Germany) and NEBNext Multiplex Oligos for Illumina (Dual Index Primers) to selectively enrich library fragments. The PCR products were purified twice using NucleoMag SPRI beads, and the quality of the final library was assessed on the Labchip GX II bioanalyzer. Indexed and purified libraries were sequenced on the Illumina NextSeq 500 platform (paired-end, 2 × 75 bp per read).

Exploratory transcriptomic analysis. High-throughput RNA sequencing (RNA-seq) was performed in duplicate on a collection of 33 isolates with independently grown bacterial cells. These 33 isolates were selected to represent the variety of LT values and distribution of lineages, clonal complexes (CCs), and origins in the original isolate collection. Sequencing quality was assessed using FastQC, and Illumina adapter sequences and low-quality base pairs were removed using cutadapt version 1.9 (80). Reads were further trimmed in 3′ using the sickle program version 1.33 with option -x and default values for all other parameters (implying a Phred quality cutoff of 20). The cleaned reads were then mapped against the whole repertoire of allelic variants for the 2,867 CDSs annotated in strain EGDe found in the 33 genomes using bowtie2 version 2.2.6 (81) with the options "-N 1 -L 16 -R 4" and converted to bam format using SAMtools version 1.9 (82). Read counts on each allelic variant were obtained using HTSeq-count version 0.10.0 (83) with options "-s reverse --nonunique all -a 1." Read counts associated with all allelic variants were summed up to obtain a single read count per gene per sample. Importantly, bowtie2 as used here mapped each read on a single allelic variant, ensuring that each read could not be counted more than once and "htseq-count" options allowed us to retrieve the reads that mapped equally well on several sequences as expected given the redundancy of the repertoire of allelic variants.

All subsequent analyses and graphical representations were conducted with R. Read counts were normalized with the function "estimateSizeFactors" provided in the R package DESeq2 (84) version 1.20.0 based on the behavior of the 2,456 conserved single-copy genes (option "controlGenes") and expressed as rpkm (reads per kilobase per million mapped reads) using the median number of reads aligned on conserved single-copy genes as the library size. Expression levels were converted to $\log_2$ scale after adding a pseudocount of 10 which corresponded approximately to the 10% quantile of rpkm values obtained for the conserved single-copy genes.

Principal-component analysis (PCA) used function "prcomp" in R package "stats" on centered but nonscaled variables corresponding to the expression values in $\log_2$ scale, i.e., $\log_2$ (rpkm + 10). Hierarchical clustering analyses were performed with function "hclust" in R package "stats" using average link aggregation method based on Pearson distance ($1 - r$ where r is the pairwise correlation coefficient). Pearson and Spearman's rank correlation coefficients (denoted as r and ρ, respectively) as well as the P values associated with the PCs presented in Fig. 5B and C were obtained with function "cor" in R. Heatmaps were drawn with function "heatmap.2" provided by R package "gplots." Quantiles corresponding to the values of ρ under the null hypothesis of no statistical association between transcript levels and isolate characteristics (lineage, Maury's classification of genotypes, and LT50) were obtained by 25,000 random permutations of isolate labels that preserved the correlation between biological replicates. Quantiles were converted to P values of a two-sided test designed to reject the null hypothesis of random association by applying the transformation $1–2|x - 0.5|$. These P values served to estimate the false-discovery rates (q values) using the R function fdrtool version 1.2.15 (85).

The functional classification was downloaded from ListiList (http://genolist.pasteur.fr/ListiList/) which consists of 43 functional categories, including three noninformative classes (unknown protein functions) for genes found in *L. monocytogenes* EGDe.

Accession number(s). The RNA-seq data sets generated for this study can be found in the Gene Expression Omnibus under accession no. GSE129537.

SUPPLEMENTAL MATERIAL

Supplemental material for this article may be found at https://doi.org/10.1128/AEM.01370-19.

SUPPLEMENTAL FILE 1, PDF file, 0.3 MB.
SUPPLEMENTAL FILE 2, XLSX file, 0.6 MB.
SUPPLEMENTAL FILE 3, XLSX file, 5.6 MB.
SUPPLEMENTAL FILE 4, XLSX file, 0.6 MB.
SUPPLEMENTAL FILE 5, XLSX file, 0.7 MB.
SUPPLEMENTAL FILE 6, XLSX file, 0.6 MB.

ACKNOWLEDGMENTS

We are grateful to Jean-Francois Bernardet at INRA, Jouy-en-Josas, France, for critically reading the manuscript. We thank Susan Joyce and Cormac Gahan at University College Cork, Ireland for training in *G. mellonella* model of infection. We greatly acknowledge Sophie Roussel at INRA, Rennes, France, Benjamin Felix and Michel-Yves Mistou at Anses, Maisons-Alfort, France, Taran Skjerdal at Norwegian Veterinary Institute, Oslo, Norway, and Carole Feurer at The French Pork and Pig Institute, Maisons-Alfort, France, for kindly providing *L. monocytogenes* isolates. Special thanks to Nicolas Krezdorn in GenXPro for genome assembly. We are grateful to the INRA MIGALE bioinformatics platform for providing computational resources.

This project received funding from the European Union's Horizon 2020 research and innovation program under Marie Skłodowska-Curie grant agreement 641984.

B.-H. Lee, P. Nicolas, and P. Piveteau conceived the project. L. Gal, D. Garmyn, and B.-H. Lee performed *in vivo* and *in vitro* experiments. C. Guérin processed the RNA-seq raw data. B.-H. Lee and P. Nicolas performed analysis of the data and interpreted the results. L. Guillier provided isolates with genome sequences. A. Rico and B. Rotter guided the RNA-seq library preparation carried out by B.-H. Lee. B.-H. Lee, P. Nicolas, and P. Piveteau wrote the manuscript, and all authors reviewed and approved the final version of the manuscript.

REFERENCES

1. Leclercq A, Moura A, Vales G, Tessaud-Rita N, Aguilhon C, Lecuit M. 2019. *Listeria thailandensis* sp. nov. Int J Syst Evol Microbiol 69:74–81. https://doi.org/10.1099/ijsem.0.003097.
2. Orsi RH, Wiedmann M. 2016. Characteristics and distribution of *Listeria* spp., including *Listeria* species newly described since 2009. Appl Microbiol Biotechnol 100:5273–5287. https://doi.org/10.1007/s00253-016-7552-2.
3. Sauders BD, Overdevest J, Fortes E, Windham K, Schukken Y, Lembo A, Wiedmann M. 2012. Diversity of *Listeria* species in urban and natural environments. Appl Environ Microbiol 78:4420–4433. https://doi.org/10.1128/AEM.00282-12.
4. Vivant A-L, Garmyn D, Piveteau P. 2013. *Listeria monocytogenes*, a down-to-earth pathogen. Front Cell Infect Microbiol 3:87. https://doi.org/10.3389/fcimb.2013.00087.
5. Radoshevich L, Cossart P. 2018. *Listeria monocytogenes*: towards a complete picture of its physiology and pathogenesis. Nat Rev Microbiol 16:32–46. https://doi.org/10.1038/nrmicro.2017.126.
6. Buchanan RL, Gorris LGM, Hayman MM, Jackson TC, Whiting RC. 2017. A review of *Listeria monocytogenes*: an update on outbreaks, virulence, dose-response, ecology, and risk assessments. Food Control 75:1–13. https://doi.org/10.1016/j.foodcont.2016.12.016.
7. Charlier C, Perrodeau É, Leclercq A, Cazenave B, Pilmis B, Henry B, Lopes A, Maury MM, Moura A, Goffinet F, Dieye HB, Thouvenot P, Ungeheuer M-N, Tourdjman M, Goulet V, de Valk H, Lortholary O, Ravaud P, Lecuit M, MONALISA Study Group. 2017. Clinical features and prognostic factors of listeriosis: the MONALISA national prospective cohort study. Lancet Infect Dis 17:510–519. https://doi.org/10.1016/S1473-3099(16)30521-7.
8. Orsi RH, den Bakker HC, Wiedmann M. 2011. *Listeria monocytogenes* lineages: genomics, evolution, ecology, and phenotypic characteristics. Int J Med Microbiol 301:79–96. https://doi.org/10.1016/j.ijmm.2010.05.002.
9. Ward TJ, Ducey TF, Usgaard T, Dunn KA, Bielawski JP. 2008. Multilocus genotyping assays for single nucleotide polymorphism-based subtyping of *Listeria monocytogenes* isolates. Appl Environ Microbiol 74:7629–7642. https://doi.org/10.1128/AEM.01127-08.
10. Ragon M, Wirth T, Hollandt F, Lavenir R, Lecuit M, Monnier AL, Brisse S. 2008. A new perspective on *Listeria monocytogenes* evolution. PLoS Pathog 4:e1000146. https://doi.org/10.1371/journal.ppat.1000146.
11. Maury MM, Tsai Y-H, Charlier C, Touchon M, Chenal-Francisque V, Leclercq A, Criscuolo A, Gaultier C, Roussel S, Brisabois A, Disson O, Rocha EPC, Brisse S, Lecuit M. 2016. Uncovering *Listeria monocytogenes* hypervirulence by harnessing its biodiversity. Nat Genet 48:308–313. https://doi.org/10.1038/ng.3501.
12. Painset A, Björkman JT, Kiil K, Guillier L, Mariet J-F, Félix B, Amar C, Rotariu O, Roussel S, Perez-Reche F, Brisse S, Moura A, Lecuit M, Forbes K, Strachan N, Grant K, Møller-Nielsen E, Dallman TJ. 2019. LiSEQ — whole-genome sequencing of a cross-sectional survey of *Listeria monocytogenes* in ready-to-eat foods and human clinical cases in Europe. Microb Genom 5:e000257. https://doi.org/10.1099/mgen.0.000257.
13. Fritsch L, Guillier L, Augustin J-C. 2018. Next generation quantitative microbiological risk assessment: refinement of the cold smoked salmon-related listeriosis risk model by integrating genomic data. Microb Risk Anal 10:20–27. https://doi.org/10.1016/j.mran.2018.06.003.
14. Rahman A, Munther D, Fazil A, Smith B, Wu J. 2018. Advancing risk assessment: mechanistic dose-response modelling of *Listeria monocytogenes* infection in human populations. R Soc Open Sci 5:180343. https://doi.org/10.1098/rsos.180343.

15. Zhang T, Abel S, Abel Zur Wiesch P, Sasabe J, Davis BM, Higgins DE, Waldor MK. 2017. Deciphering the landscape of host barriers to *Listeria monocytogenes* infection. Proc Natl Acad Sci U S A 114:6334–6339. https://doi.org/10.1073/pnas.1702077114.
16. Cossart P. 2011. Illuminating the landscape of host–pathogen interactions with the bacterium *Listeria monocytogenes*. Proc Natl Acad Sci U S A 108:19484–19491. https://doi.org/10.1073/pnas.1112371108.
17. Glaser P, Frangeul L, Buchrieser C, Rusniok C, Amend A, Baquero F, Berche P, Bloecker H, Brandt P, Chakraborty T, Charbit A, Chetouani F, Couvé E, de Daruvar A, Dehoux P, Domann E, Domínguez-Bernal G, Duchaud E, Durant L, Dussurget O, Entian KD, Fsihi H, García-del Portillo F, Garrido P, Gautier L, Goebel W, Gómez-López N, Hain T, Hauf J, Jackson D, Jones LM, Kaerst U, Kreft J, Kuhn M, Kunst F, Kurapkat G, Madueno E, Maitournam A, Vicente JM, Ng E, Nedjari H, Nordsiek G, Novella S, de Pablos B, Pérez-Diaz JC, Purcell R, Remmel B, Rose M, Schlueter T, Simoes N, Tierrez A, Vázquez-Boland JA, Voss H, Wehland J, Cossart P. 2001. Comparative genomics of *Listeria* species. Science 294:849–852.
18. Clayton EM, Daly KM, Guinane CM, Hill C, Cotter PD, Ross PR. 2014. Atypical *Listeria* innocua strains possess an intact LIPI-3. BMC Microbiol 14:58. https://doi.org/10.1186/1471-2180-14-58.
19. Vázquez-Boland JA, Domínguez-Bernal G, González-Zorn B, Kreft J, Goebel W. 2001. Pathogenicity islands and virulence evolution in *Listeria*. Microbes Infect 3:571–584. https://doi.org/10.1016/S1286-4579(01)01413-7.
20. Cotter PD, Draper LA, Lawton EM, Daly KM, Groeger DS, Casey PG, Ross RP, Hill C. 2008. Listeriolysin S, a novel peptide haemolysin associated with a subset of lineage I *Listeria monocytogenes*. PLoS Pathog 4:e1000144. https://doi.org/10.1371/journal.ppat.1000144.
21. Hadorn K, Hächler H, Schaffner A, Kayser FH. 1993. Genetic characterization of plasmid-encoded multiple antibiotic resistance in a strain of *Listeria monocytogenes* causing endocarditis. Eur J Clin Microbiol Infect Dis 12:928–937. https://doi.org/10.1007/BF01992167.
22. Poyart-Salmeron C, Carlier C, Trieu-Cuot P, Courvalin P, Courtieu A-L. 1990. Transferable plasmid-mediated antibiotic resistance in *Listeria monocytogenes*. Lancet 335:1422–1426. https://doi.org/10.1016/0140-6736(90)91447-I.
23. den Bakker HC, Bowen BM, Rodriguez-Rivera LD, Wiedmann M. 2012. FSL J1-208, a virulent uncommon phylogenetic lineage IV *Listeria monocytogenes* strain with a small chromosome size and a putative virulence plasmid carrying internalin-like genes. Appl Environ Microbiol 78:1876–1889. https://doi.org/10.1128/AEM.06969-11.
24. Toledo-Arana A, Dussurget O, Nikitas G, Sesto N, Guet-Revillet H, Balestrino D, Loh E, Gripenland J, Tiensuu T, Vaitkevicius K, Barthelemy M, Vergassola M, Nahori M-A, Soubigou G, Régnault B, Coppée J-Y, Lecuit M, Johansson J, Cossart P. 2009. The *Listeria* transcriptional landscape from saprophytism to virulence. Nature 459:950–956. https://doi.org/10.1038/nature08080.
25. Lebreton A, Cossart P. 2017. RNA- and protein-mediated control of *Listeria monocytogenes* virulence gene expression. RNA Biol 14:460–470. https://doi.org/10.1080/15476286.2016.1189069.
26. Bécavin C, Bouchier C, Lechat P, Archambaud C, Creno S, Gouin E, Wu Z, Kühbacher A, Brisse S, Pucciarelli MG, García-del Portillo F, Hain T, Portnoy DA, Chakraborty T, Lecuit M, Pizarro-Cerdá J, Moszer I, Bierne H, Cossart P. 2014. Comparison of widely used *Listeria monocytogenes* strains EGD, 10403S, and EGD-e highlights genomic variations underlying differences in pathogenicity. mBio 5:e00969-14. https://doi.org/10.1128/mBio.00969-14.
27. Cerutti F, Mallet L, Painset A, Hoede C, Moisan A, Bécavin C, Duval M, Dussurget O, Cossart P, Gaspin C, Chiapello H. 2017. Unraveling the evolution and coevolution of small regulatory RNAs and coding genes in *Listeria*. BMC Genomics 18:882. https://doi.org/10.1186/s12864-017-4242-0.
28. Maury MM, Chenal-Francisque V, Bracq-Dieye H, Han L, Leclercq A, Vales G, Moura A, Gouin E, Scortti M, Disson O, Vázquez-Boland JA, Lecuit M. 2017. Spontaneous loss of virulence in natural populations of *Listeria monocytogenes*. Infect Immun 85:e00541-17. https://doi.org/10.1128/IAI.00541-17.
29. Olier M, Pierre F, Rousseaux S, Lemaître J-P, Rousset A, Piveteau P, Guzzo J. 2003. Expression of truncated internalin A is involved in impaired internalization of some *Listeria monocytogenes* isolates carried asymptomatically by humans. Infect Immun 71:1217–1224. https://doi.org/10.1128/iai.71.3.1217-1224.2003.
30. Port GC, Freitag NE. 2007. Identification of novel *Listeria monocytogenes* secreted virulence factors following mutational activation of the central virulence regulator, PrfA. Infect Immun 75:5886–5897. https://doi.org/10.1128/IAI.00845-07.
31. Rousseaux S, Olier M, Lemaître JP, Piveteau P, Guzzo J. 2004. Use of PCR-restriction fragment length polymorphism of *inlA* for rapid screening of *Listeria monocytogenes* strains deficient in the ability to invade Caco-2 cells. Appl Environ Microbiol 70:2180–2185. https://doi.org/10.1128/AEM.70.4.2180-2185.2004.
32. Liu D, Lawrence ML, Austin FW, Ainsworth AJ. 2007. A multiplex PCR for species- and virulence-specific determination of *Listeria monocytogenes*. J Microbiol Methods 71:133–140. https://doi.org/10.1016/j.mimet.2007.08.007.
33. Olier M, Garmyn D, Rousseaux S, Lemaître J-P, Piveteau P, Guzzo J. 2005. Truncated internalin A and asymptomatic *Listeria monocytogenes* carriage: *in vivo* investigation by allelic exchange. Infect Immun 73:644–648. https://doi.org/10.1128/IAI.73.1.644-648.2005.
34. Roberts AJ, Williams SK, Wiedmann M, Nightingale KK. 2009. Some *Listeria monocytogenes* outbreak strains demonstrate significantly reduced invasion, *inlA* transcript levels, and swarming motility *in vitro*. Appl Environ Microbiol 75:5647–5658. https://doi.org/10.1128/AEM.00367-09.
35. Scortti M, Han L, Alvarez S, Leclercq A, Moura A, Lecuit M, Vazquez-Boland J. 2018. Epistatic control of intrinsic resistance by virulence genes in *Listeria*. PLoS Genet 14:e1007525. https://doi.org/10.1371/journal.pgen.1007727.
36. Camejo A, Buchrieser C, Couvé E, Carvalho F, Reis O, Ferreira P, Sousa S, Cossart P, Cabanes D. 2009. *In vivo* transcriptional profiling of *Listeria monocytogenes* and mutagenesis identify new virulence factors involved in infection. PLoS Pathog 5:e1000449. https://doi.org/10.1371/journal.pgen.1007525.
37. Autret N, Raynaud C, Dubail I, Berche P, Charbit A. 2003. Identification of the agr locus of *Listeria monocytogenes*: role in bacterial virulence. Infect Immun 71:4463–4471. https://doi.org/10.1128/iai.71.8.4463-4471.2003.
38. Kazmierczak MJ, Mithoe SC, Boor KJ, Wiedmann M. 2003. *Listeria monocytogenes* σB regulates stress response and virulence functions. J Bacteriol 185:5722–5734. https://doi.org/10.1128/JB.185.19.5722-5734.2003.
39. Nadon CA, Bowen BM, Wiedmann M, Boor KJ. 2002. Sigma B contributes to PrfA-mediated virulence in *Listeria monocytogenes*. Infect Immun 70:3948–3952. https://doi.org/10.1128/iai.70.7.3948-3952.2002.
40. Wurtzel O, Sesto N, Mellin JR, Karunker I, Edelheit S, Bécavin C, Archambaud C, Cossart P, Sorek R. 2012. Comparative transcriptomics of pathogenic and non-pathogenic *Listeria* species. Mol Syst Biol 8:583. https://doi.org/10.1038/msb.2012.11.
41. Severino P, Dussurget O, Vêncio RZN, Dumas E, Garrido P, Padilla G, Piveteau P, Lemaître J-P, Kunst F, Glaser P, Buchrieser C. 2007. Comparative transcriptome analysis of *Listeria monocytogenes* strains of the two major lineages reveals differences in virulence, cell wall, and stress response. Appl Environ Microbiol 73:6078–6088. https://doi.org/10.1128/AEM.02730-06.
42. Couto N, Belas A, Oliveira M, Almeida P, Clemente C, Pomba C. 2016. Comparative RNA-seq-based transcriptome analysis of the virulence characteristics of methicillin-resistant and -susceptible *Staphylococcus pseudintermedius* strains isolated from small animals. Antimicrob Agents Chemother 60:962–967. https://doi.org/10.1128/AAC.01907-15.
43. Biller L, Davis PH, Tillack M, Matthiesen J, Lotter H, Stanley SL, Tannich E, Bruchhaus I. 2010. Differences in the transcriptome signatures of two genetically related *Entamoeba histolytica* cell lines derived from the same isolate with different pathogenic properties. BMC Genomics 11:63. https://doi.org/10.1186/1471-2164-11-63.
44. Gahan CGM, Hill C. 2014. *Listeria monocytogenes*: survival and adaptation in the gastrointestinal tract. Front Cell Infect Microbiol 4:9. https://doi.org/10.3389/fcimb.2014.00009.
45. Strimmer K. 2008. A unified approach to false discovery rate estimation. BMC Bioinformatics 9:303. https://doi.org/10.1186/1471-2105-9-303.
46. Chaturongakul S, Raengpradub S, Palmer ME, Bergholz TM, Orsi RH, Hu Y, Ollinger J, Wiedmann M, Boor KJ. 2011. Transcriptomic and phenotypic analyses identify coregulated, overlapping regulons among PrfA, CtsR, HrcA, and the alternative sigma factors sigmaB, sigmaC, sigmaH, and sigmaL in *Listeria monocytogenes*. Appl Environ Microbiol 77:187–200. https://doi.org/10.1128/AEM.00952-10.
47. Palmer ME, Chaturongakul S, Wiedmann M, Boor KJ. 2011. The *Listeria monocytogenes* σB regulon and its virulence-associated functions are inhibited by a small molecule. mBio 2:e00241-11. https://doi.org/10.1128/mBio.00241-11.
48. Hu Y, Raengpradub S, Schwab U, Loss C, Orsi RH, Wiedmann M, Boor KJ.

2007. Phenotypic and transcriptomic analyses demonstrate interactions between the transcriptional regulators CtsR and Sigma B in *Listeria monocytogenes*. Appl Environ Microbiol 73:7967–7980. https://doi.org/10.1128/AEM.01085-07.
49. Bennett HJ, Pearce DM, Glenn S, Taylor CM, Kuhn M, Sonenshein AL, Andrew PW, Roberts IS. 2007. Characterization of relA and codY mutants of *Listeria monocytogenes*: identification of the CodY regulon and its role in virulence. Mol Microbiol 63:1453–1467. https://doi.org/10.1111/j.1365-2958.2007.05597.x.
50. Mandin P, Fsihi H, Dussurget O, Vergassola M, Milohanic E, Toledo-Arana A, Lasa I, Johansson J, Cossart P. 2005. VirR, a response regulator critical for *Listeria monocytogenes* virulence. Mol Microbiol 57:1367–1380. https://doi.org/10.1111/j.1365-2958.2005.04776.x.
51. Scortti M, Monzó HJ, Lacharme-Lora L, Lewis DA, Vázquez-Boland JA. 2007. The PrfA virulence regulon. Microbes Infect 9:1196–1207. https://doi.org/10.1016/j.micinf.2007.05.007.
52. Novichkov PS, Kazakov AE, Ravcheev DA, Leyn SA, Kovaleva GY, Sutormin RA, Kazanov MD, Riehl W, Arkin AP, Dubchak I, Rodionov DA. 2013. RegPrecise 3.0–a resource for genome-scale exploration of transcriptional regulation in bacteria. BMC Genomics 14:745. https://doi.org/10.1186/1471-2164-14-745.
53. Zimmermann L, Stephens A, Nam S-Z, Rau D, Kübler J, Lozajic M, Gabler F, Söding J, Lupas AN, Alva V. 2018. A completely reimplemented MPI bioinformatics toolkit with a new HHpred server at its core. J Mol Biol 430:2237–2243. https://doi.org/10.1016/j.jmb.2017.12.007.
54. Schauer K, Geginat G, Liang C, Goebel W, Dandekar T, Fuchs TM. 2010. Deciphering the intracellular metabolism of *Listeria monocytogenes* by mutant screening and modelling. BMC Genomics 11:573. https://doi.org/10.1186/1471-2164-11-573.
55. Guinane CM, Cotter PD, Ross RP, Hill C. 2006. Contribution of penicillin-binding protein homologs to antibiotic resistance, cell morphology, and virulence of *Listeria monocytogenes* EGDe. Antimicrob Agents Chemother 50:2824–2828. https://doi.org/10.1128/AAC.00167-06.
56. Shimizu K. 2013. Regulation systems of bacteria such as *Escherichia coli* in response to nutrient limitation and environmental stresses. Metabolites 4:1–35. https://doi.org/10.3390/metabo4010001.
57. Price AL, Patterson NJ, Plenge RM, Weinblatt ME, Shadick NA, Reich D. 2006. Principal components analysis corrects for stratification in genome-wide association studies. Nat Genet 38:904–909. https://doi.org/10.1038/ng1847.
58. Price AL, Zaitlen NA, Reich D, Patterson N. 2010. New approaches to population stratification in genome-wide association studies. Nat Rev Genet 11:459–463. https://doi.org/10.1038/nrg2813.
59. Ribet D, Cossart P. 2010. Post-translational modifications in host cells during bacterial infection. FEBS Lett 584:2748–2758. https://doi.org/10.1016/j.febslet.2010.05.012.
60. Scully LR, Bidochka MJ. 2006. Developing insect models for the study of current and emerging human pathogens. FEMS Microbiol Lett 263:1–9. https://doi.org/10.1111/j.1574-6968.2006.00388.x.
61. Joyce SA, Gahan C. 2010. Molecular pathogenesis of *Listeria monocytogenes* in the alternative model host *Galleria mellonella*. Microbiology 156:3456–3468. https://doi.org/10.1099/mic.0.040782-0.
62. Mukherjee K, Altincicek B, Hain T, Domann E, Vilcinskas A, Chakraborty T. 2010. *Galleria mellonella* as a model system for studying *Listeria* pathogenesis. Appl Environ Microbiol 76:310–317. https://doi.org/10.1128/AEM.01301-09.
63. Tsai C-Y, Loh JMS, Proft T. 2016. *Galleria mellonella* infection models for the study of bacterial diseases and for antimicrobial drug testing. Virulence 7:214–229. https://doi.org/10.1080/21505594.2015.1135289.
64. Sajid A, Arora G, Singhal A, Kalia VC, Singh Y. 2015. Protein phosphatases of pathogenic bacteria: role in physiology and virulence. Annu Rev Microbiol 69:527–547. https://doi.org/10.1146/annurev-micro-020415-111342.
65. Rameshwaram NR, Singh P, Ghosh S, Mukhopadhyay S. 2018. Lipid metabolism and intracellular bacterial virulence: key to next-generation therapeutics. Future Microbiol 13:1301–1328. https://doi.org/10.2217/fmb-2018-0013.
66. Curtis TD, Takeuchi I, Gram L, Knudsen GM. 2017. The influence of the toxin/antitoxin mazEF on growth and survival of *Listeria monocytogenes* under stress. Toxins 9:31. https://doi.org/10.3390/toxins9010031.
67. Kalani BS, Irajian G, Lotfollahi L, Abdollahzadeh E, Razavi S. 2018. Putative type II toxin-antitoxin systems in *Listeria monocytogenes* isolated from clinical, food, and animal samples in Iran. Microb Pathog 122:19–24. https://doi.org/10.1016/j.micpath.2018.06.003.
68. Rabinovich L, Sigal N, Borovok I, Nir-Paz R, Herskovits AA. 2012. Prophage excision activates *Listeria* competence genes that promote phagosomal escape and virulence. Cell 150:792–802. https://doi.org/10.1016/j.cell.2012.06.036.
69. Beceiro A, Tomás M, Bou G. 2013. Antimicrobial resistance and virulence: a successful or deleterious association in the bacterial world? Clin Microbiol Rev 26:185–230. https://doi.org/10.1128/CMR.00059-12.
70. Rieux V, Carbon C, Azoulay-Dupuis E. 2001. Complex relationship between acquisition of beta-lactam resistance and loss of virulence in *Streptococcus pneumoniae*. J Infect Dis 184:66–72. https://doi.org/10.1086/320992.
71. Rudkin JK, Edwards AM, Bowden MG, Brown EL, Pozzi C, Waters EM, Chan WC, Williams P, O'Gara JP, Massey RC. 2012. Methicillin resistance reduces the virulence of healthcare-associated methicillin-resistant *Staphylococcus aureus* by interfering with the agr quorum sensing system. J Infect Dis 205:798. https://doi.org/10.1093/infdis/jir845.
72. Aké FMD, Joyet P, Deutscher J, Milohanic E. 2011. Mutational analysis of glucose transport regulation and glucose-mediated virulence gene repression in *Listeria monocytogenes*. Mol Microbiol 81:274–293. https://doi.org/10.1111/j.1365-2958.2011.07692.x.
73. Milenbachs Lukowiak A, Mueller KJ, Freitag NE, Youngman P. 2004. Deregulation of *Listeria monocytogenes* virulence gene expression by two distinct and semi-independent pathways. Microbiology 150:321–333. https://doi.org/10.1099/mic.0.26718-0.
74. Marr AK, Joseph B, Mertins S, Ecke R, Müller-Altrock S, Goebel W. 2006. Overexpression of PrfA leads to growth inhibition of *Listeria monocytogenes* in glucose-containing culture media by interfering with glucose uptake. J Bacteriol 188:3887–3901. https://doi.org/10.1128/JB.01978-05.
75. Henri C, Félix B, Guillier L, Leekitcharoenphon P, Michelon D, Mariet J-F, Aarestrup FM, Mistou M-Y, Hendriksen RS, Roussel S. 2016. Population genetic structure of *Listeria monocytogenes* strains as determined by pulsed-field gel electrophoresis and multilocus sequence typing. Appl Environ Microbiol 82:5720–5728. https://doi.org/10.1128/AEM.00583-16.
76. Bankevich A, Nurk S, Antipov D, Gurevich AA, Dvorkin M, Kulikov AS, Lesin VM, Nikolenko SI, Pham S, Prjibelski AD, Pyshkin AV, Sirotkin AV, Vyahhi N, Tesler G, Alekseyev MA, Pevzner PA. 2012. SPAdes: a new genome assembly algorithm and its applications to single-cell sequencing. J Comput Biol 19:455–477. https://doi.org/10.1089/cmb.2012.0021.
77. Camacho C, Coulouris G, Avagyan V, Ma N, Papadopoulos J, Bealer K, Madden TL. 2009. BLAST+: architecture and applications. BMC Bioinformatics 10:421. https://doi.org/10.1186/1471-2105-10-421.
78. Edgar RC. 2004. MUSCLE: multiple sequence alignment with high accuracy and high throughput. Nucleic Acids Res 32:1792–1797. https://doi.org/10.1093/nar/gkh340.
79. Guindon S, Gascuel O. 2003. A simple, fast, and accurate algorithm to estimate large phylogenies by maximum likelihood. Syst Biol 52:696–704. https://doi.org/10.1080/10635150390235520.
80. Martin M. 2011. Cutadapt removes adapter sequences from high-throughput sequencing reads. Embnet J 17:10. https://doi.org/10.14806/ej.17.1.200.
81. Langmead B, Salzberg SL. 2012. Fast gapped-read alignment with Bowtie 2. Nat Methods 9:357–359. https://doi.org/10.1038/nmeth.1923.
82. Li H, Handsaker B, Wysoker A, Fennell T, Ruan J, Homer N, Marth G, Abecasis G, Durbin R, 1000 Genome Project Data Processing Subgroup. 2009. The Sequence Alignment/Map format and SAMtools. Bioinformatics 25:2078–2079. https://doi.org/10.1093/bioinformatics/btp352.
83. Anders S, Pyl PT, Huber W. 2015. HTSeq–a Python framework to work with high-throughput sequencing data. Bioinformatics 31:166–169. https://doi.org/10.1093/bioinformatics/btu638.
84. Love MI, Huber W, Anders S. 2014. Moderated estimation of fold change and dispersion for RNA-seq data with DESeq2. Genome Biol 15:550. https://doi.org/10.1186/s13059-014-0550-8.
85. Strimmer K. 2008. fdrtool: a versatile R package for estimating local and tail area-based false discovery rates. Bioinformatics 24:1461–1462. https://doi.org/10.1093/bioinformatics/btn209.